



Advancing Asteroid Threat Assessment

Lorien Wheeler

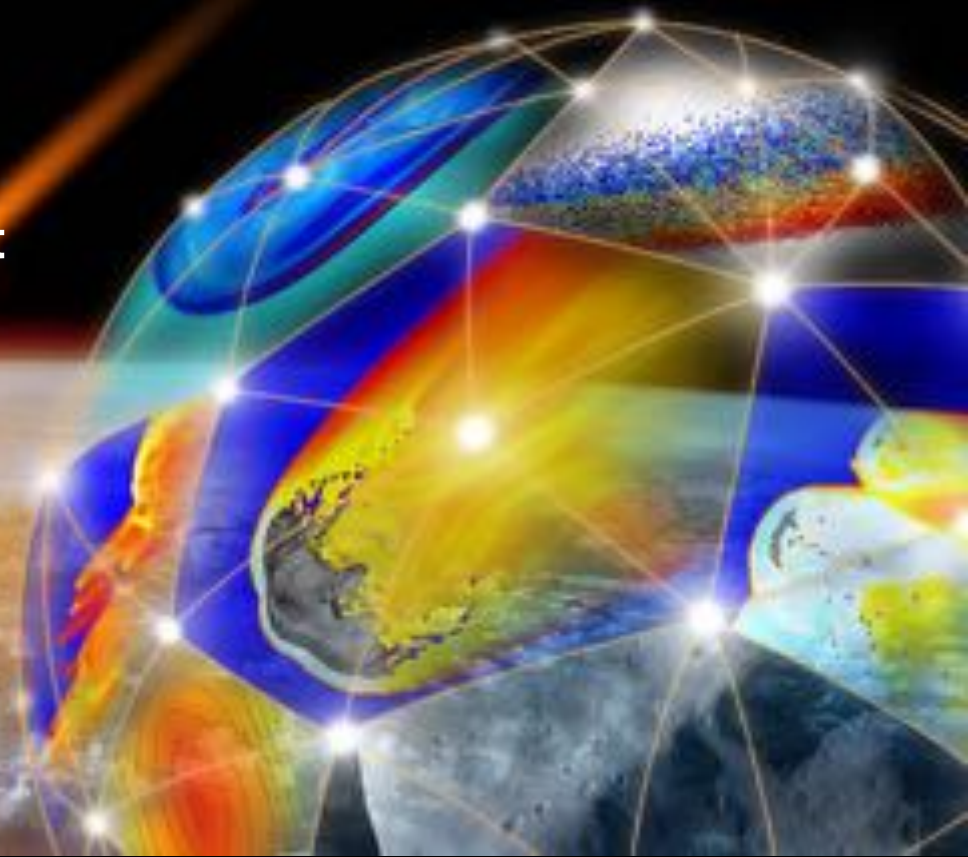
Donovan Mathias, Jessie Dotson,
Michael Aftosmis, Eric Stern,
Randy Longenbaugh

Asteroid Threat Assessment Project

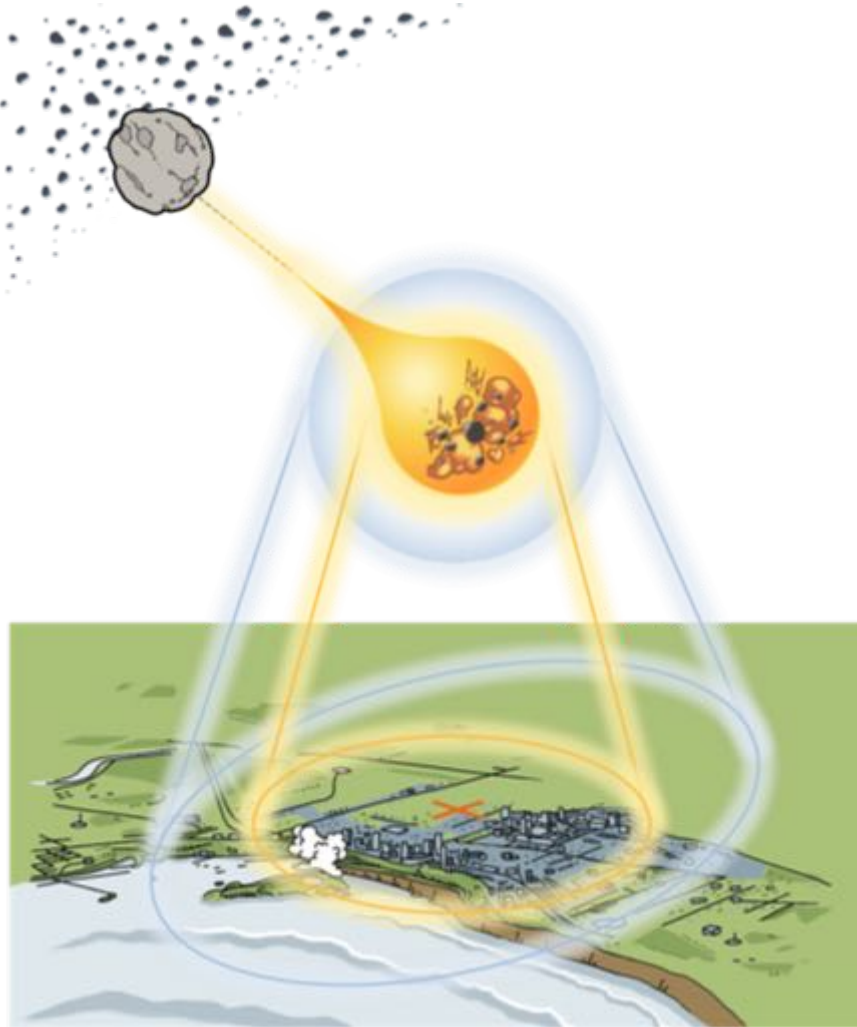
NASA Ames Research Center

Meteoroids 2019

19 June 2019, Bratislava, Slovakia



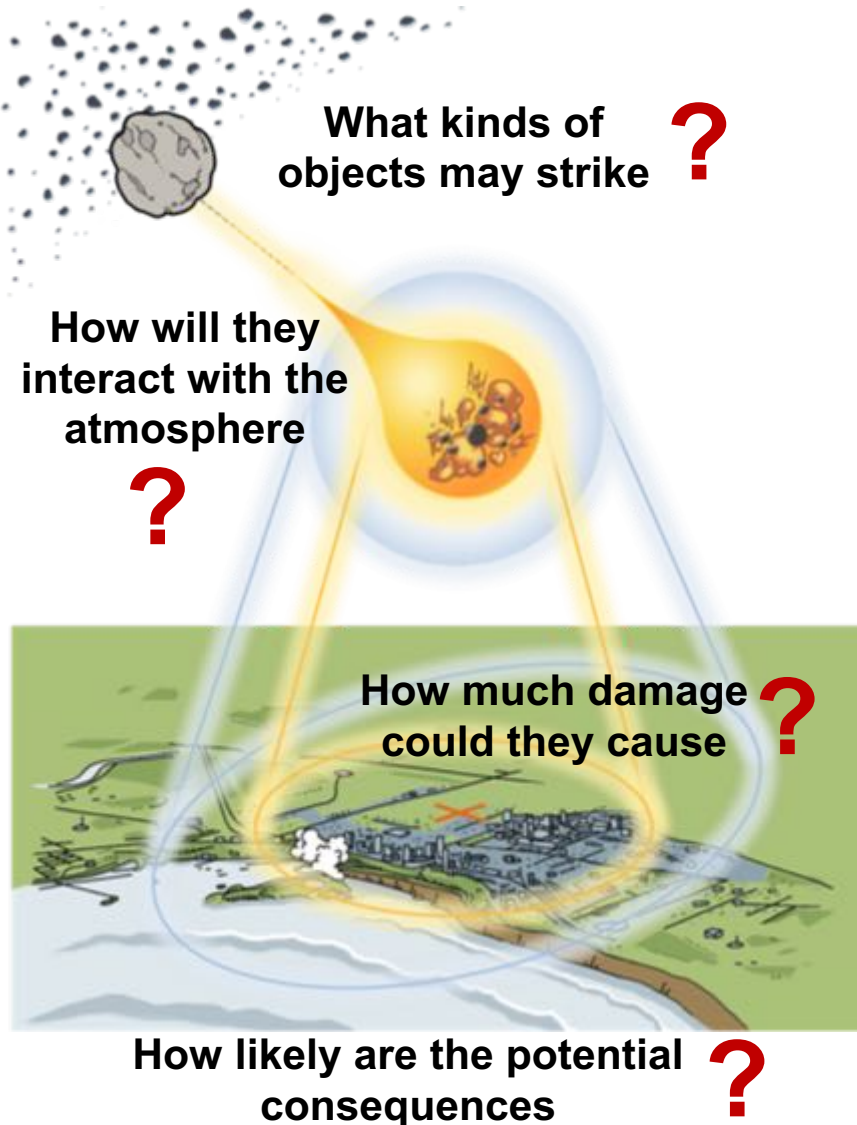
Asteroid Threat Assessment for Planetary Defense



Objectives:

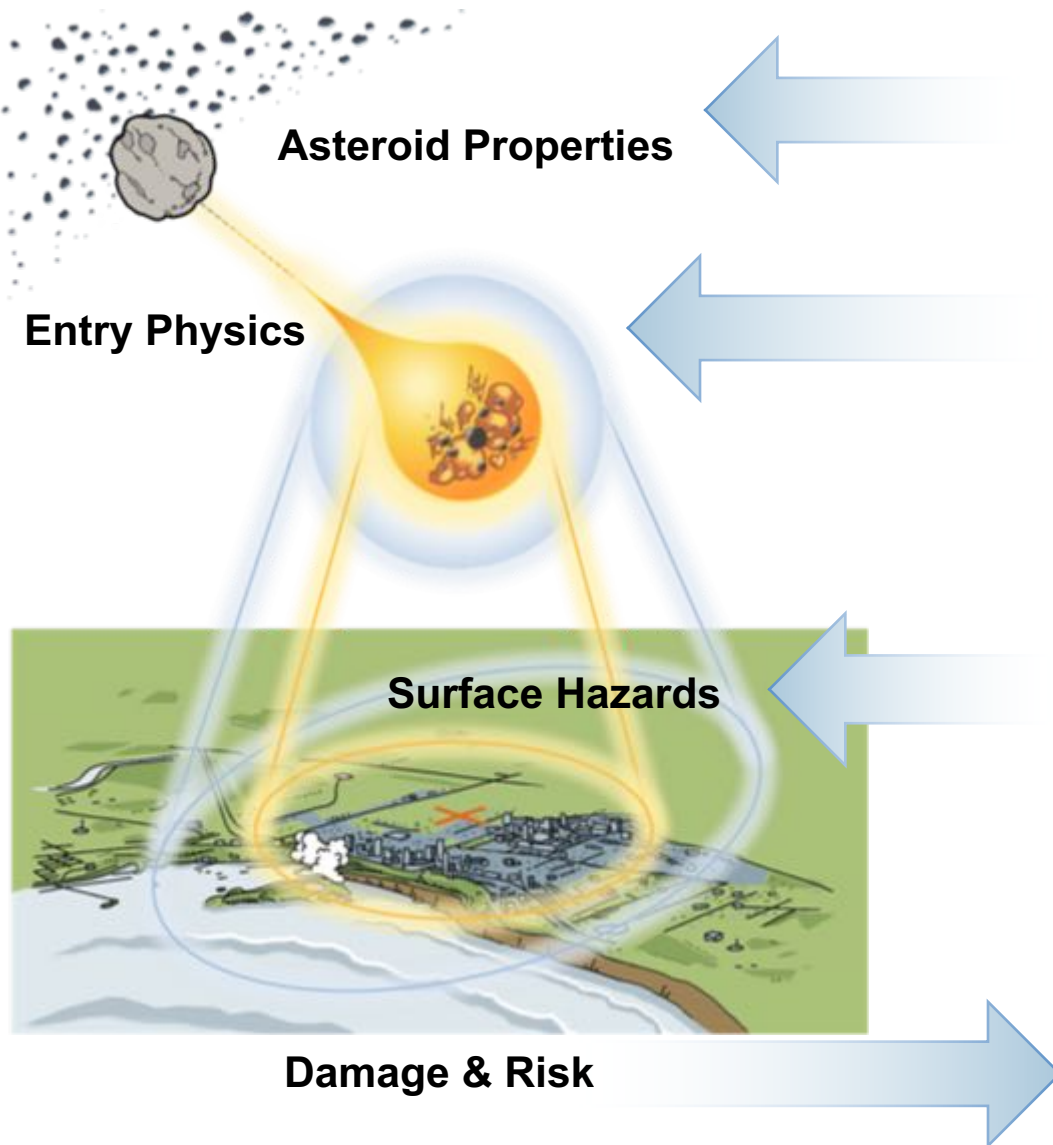
- Develop models and data to characterize the potential damage and risks due to asteroid strikes on Earth
- Provide results that can help guide decisions and planning:
 - Asteroid surveys
 - Mitigation systems
 - Disaster response

Large Uncertainties, Sparse Data



- Most observed meteor events are small and pose no threat
- Potentially hazardous objects are distant, rare, and diverse making properties difficult to characterize
- Entry & damage prediction involves complex, multi-physics processes and extreme conditions that are difficult to test

Need to extend the available data and modeling methods to much larger sizes and diverse property ranges and understand the uncertainties in doing so...



Characterization

- Meteorite measurements
- Data aggregation
- Property database website
- Inference models

Entry Simulations & Testing

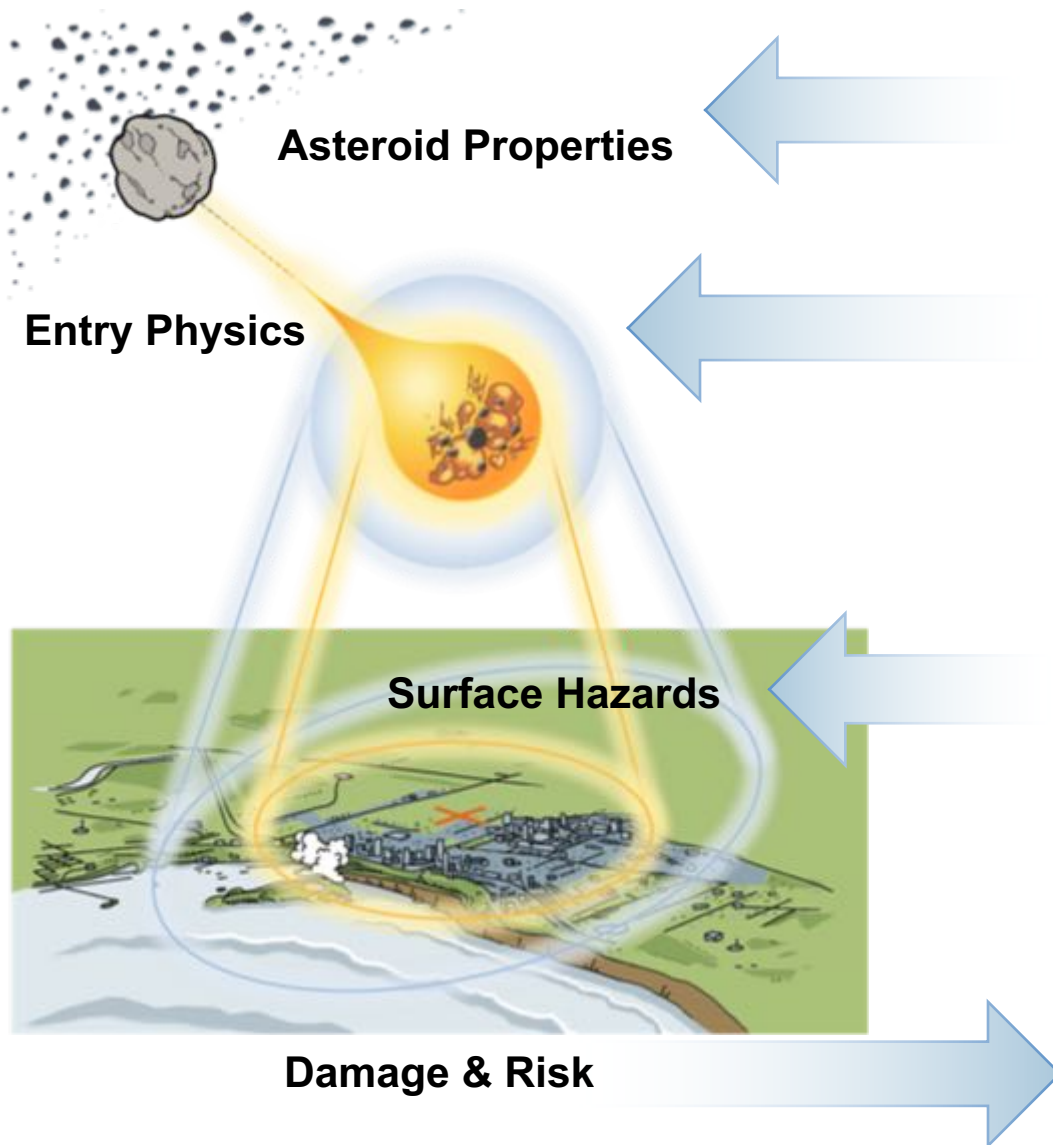
- Coupled aerothermodynamics
- Ablation & radiation modeling
- Arc jet testing

Hazard Simulations

- 3D blast simulations
- Thermal radiation models
- Impact crater simulations
- Tsunami simulations
- Global effects

Probabilistic Risk Assessment

- Fast-running physics-based entry and damage models
- Uncertainty distributions for asteroid and impact properties



Characterization

- Meteorite measurements
- Data aggregation
- Property database website
- Inference models

Entry Simulations & Testing

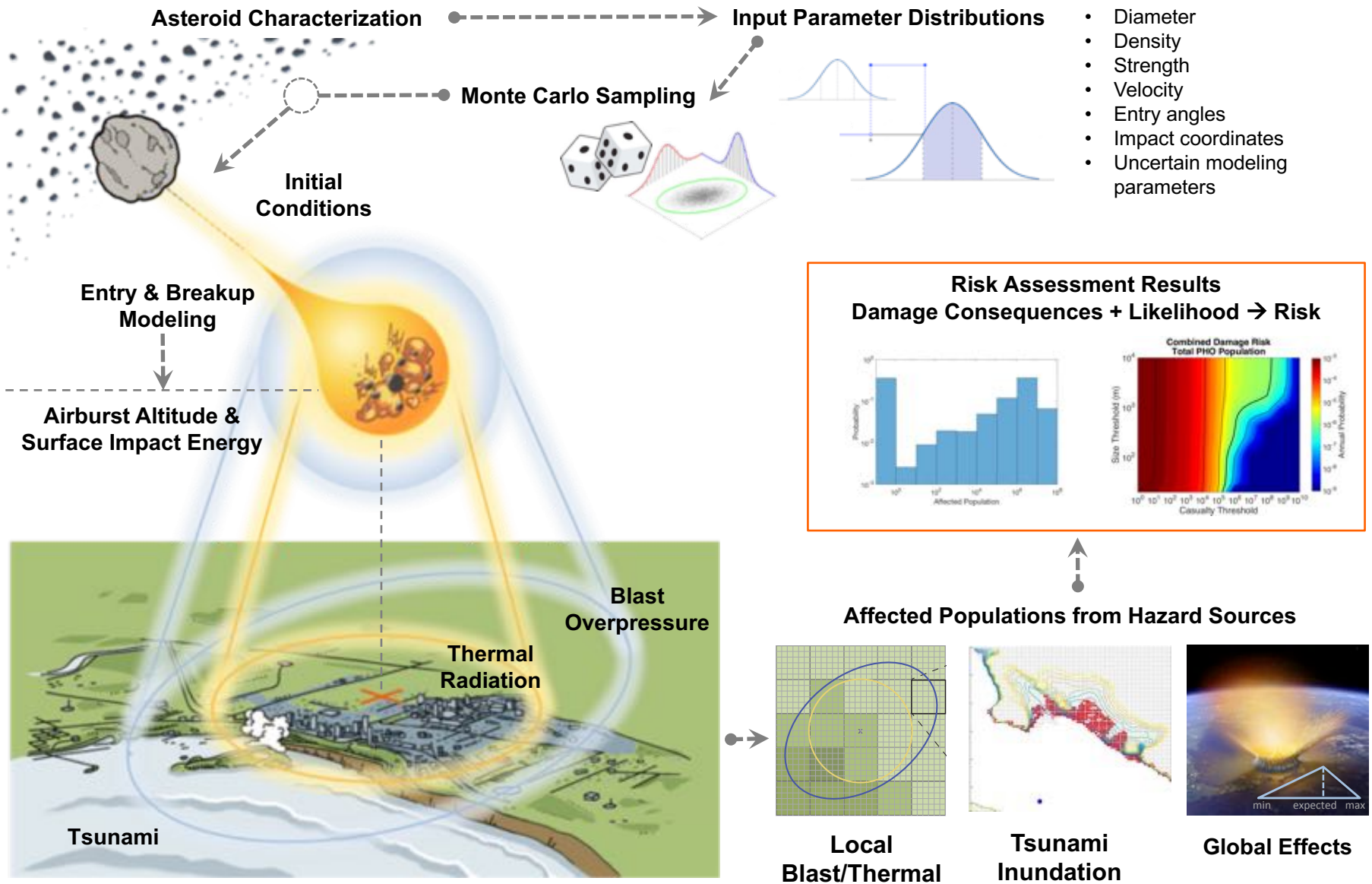
- Coupled aerothermodynamics
- Ablation & radiation modeling
- Arc jet testing

Hazard Simulations

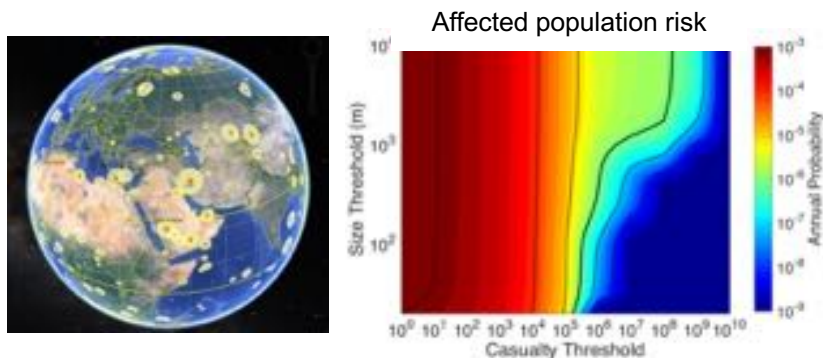
- 3D blast simulations
- Thermal radiation models
- Impact crater simulations
- Tsunami simulations
- Global effects

Probabilistic Risk Assessment

- **Fast-running physics-based entry and damage models**
- Uncertainty distributions for asteroid and impact properties

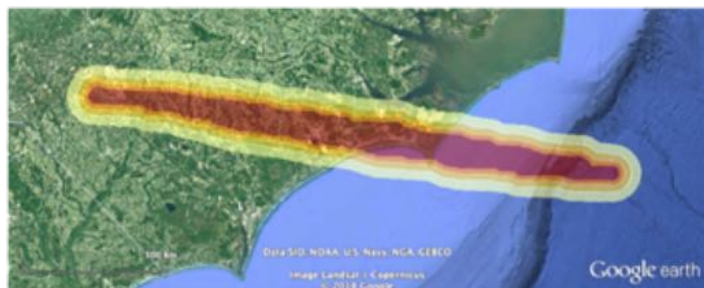


Probabilistic Risk: Consequences + Likelihood (given uncertainties)



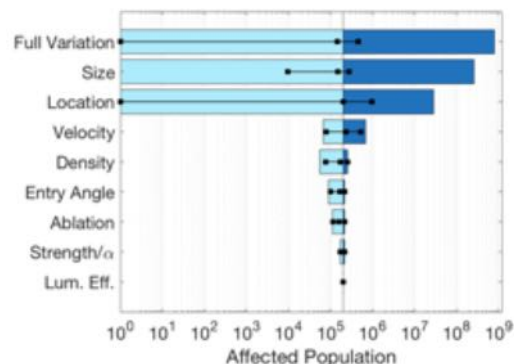
- **Ensemble risk assessments**

- Risk from general asteroid populations
- Used to inform strategic survey and mitigation planning



- **Impact scenario risk assessments**

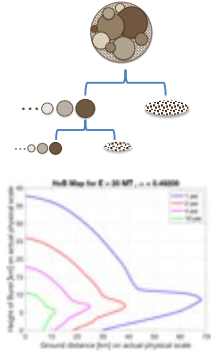
- Evaluate the threat from a specific impactor (all hypothetical so far!)
- Support disaster response planning & preparedness



- **Risk sensitivity studies**

- Identify risk-driving uncertainties
- Guide model refinements, characterization research, and asteroid missions.

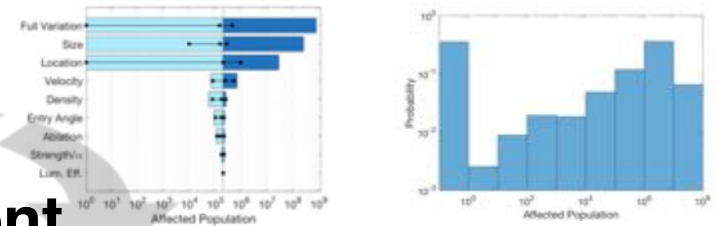
Efficient Risk Models



- Capture key risk-driving entry and damage process
- Run millions of cases
- Enable broad evaluation of potential uncertainty space.

Sensitivity Studies

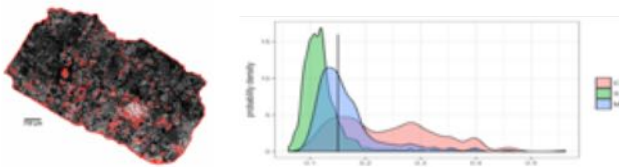
- Identify risk-driving factors
- Bound uncertainties
- Guide model refinements and characterization efforts



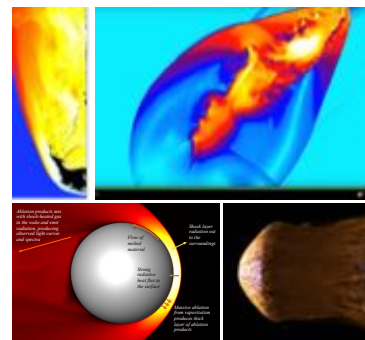
Refinement

Characterization Studies

- Refine asteroid property distributions based on sensitivity
- Characterize physical parameters appropriate for evolving models



High-fidelity Simulations & Testing



- Develop, refine, and anchor risk models and parameters
- Evaluate specific cases and processes.

Fragment-Cloud Model (FCM)

Flight integration:

$$dm/dt = -0.5 \rho_{air} v^3 A \sigma$$

$$dv/dt = \rho_{air} v^2 A C_D / m - g \sin \theta$$

$$d\theta/dt = (v / (R_E + h) - g/v) \cos \theta$$

$$dh/dt = v \sin \theta$$

Fragmentation occurs when stagnation pressure exceeds aero strength

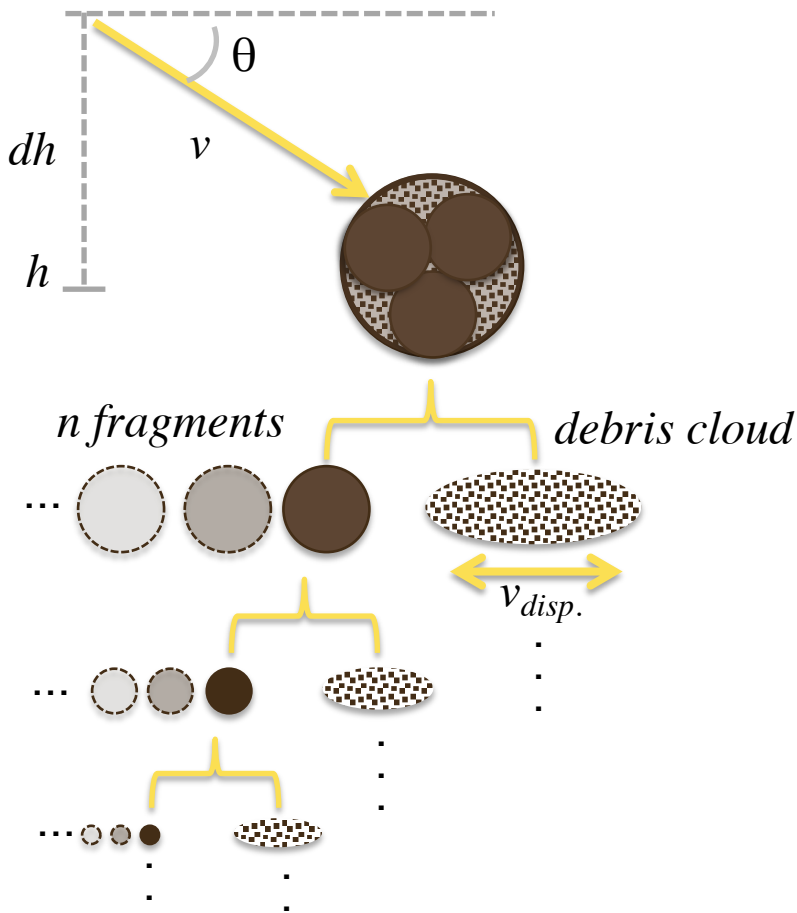
$$\rho_{air} v^2 > \text{Strength } (S)$$

Fragment strengths increase with decreased size

$$S_1 = S_0 (m_0 / m_1)^\alpha$$

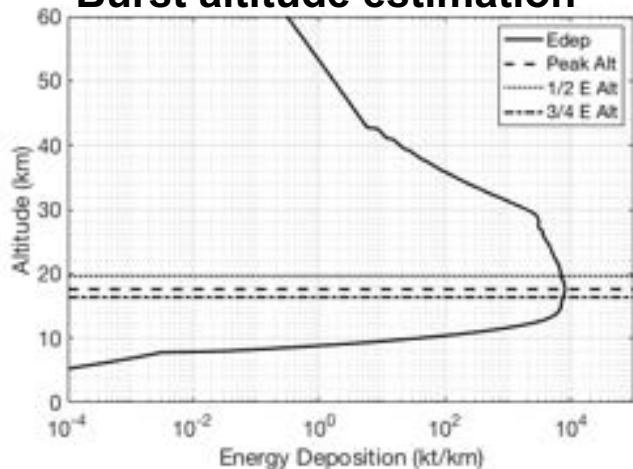
Debris clouds broaden and slow under common bow shock (“pancake” approach)

$$v_{disp.} = v_{cloud} (C_{disp} A \rho_{air} / \rho_{debris})^{1/2}$$

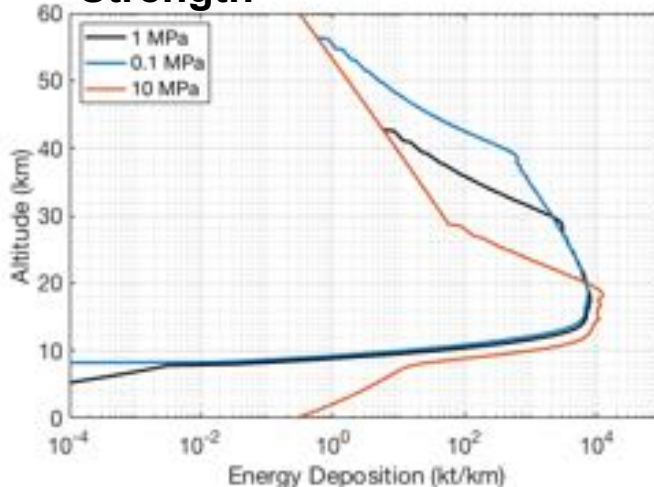


FCM Edep for Damage Modeling

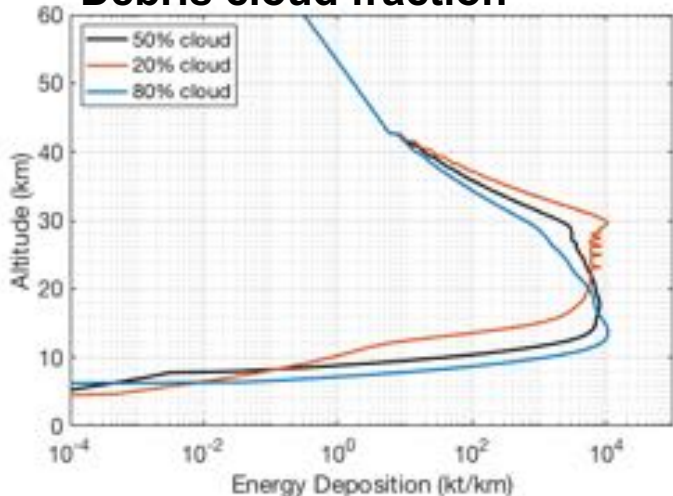
Burst altitude estimation



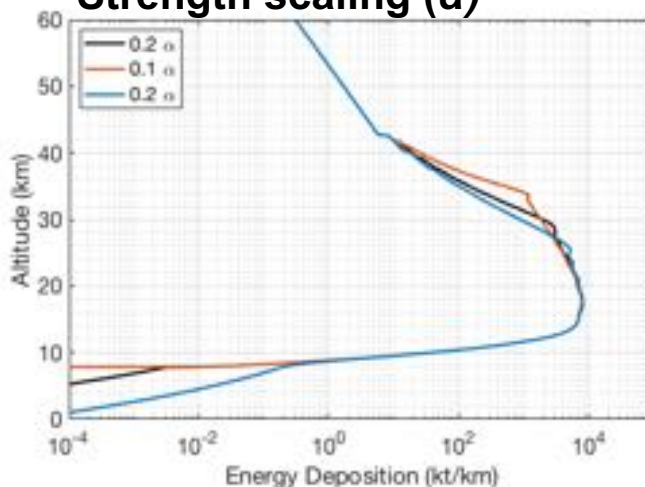
Strength



Debris cloud fraction



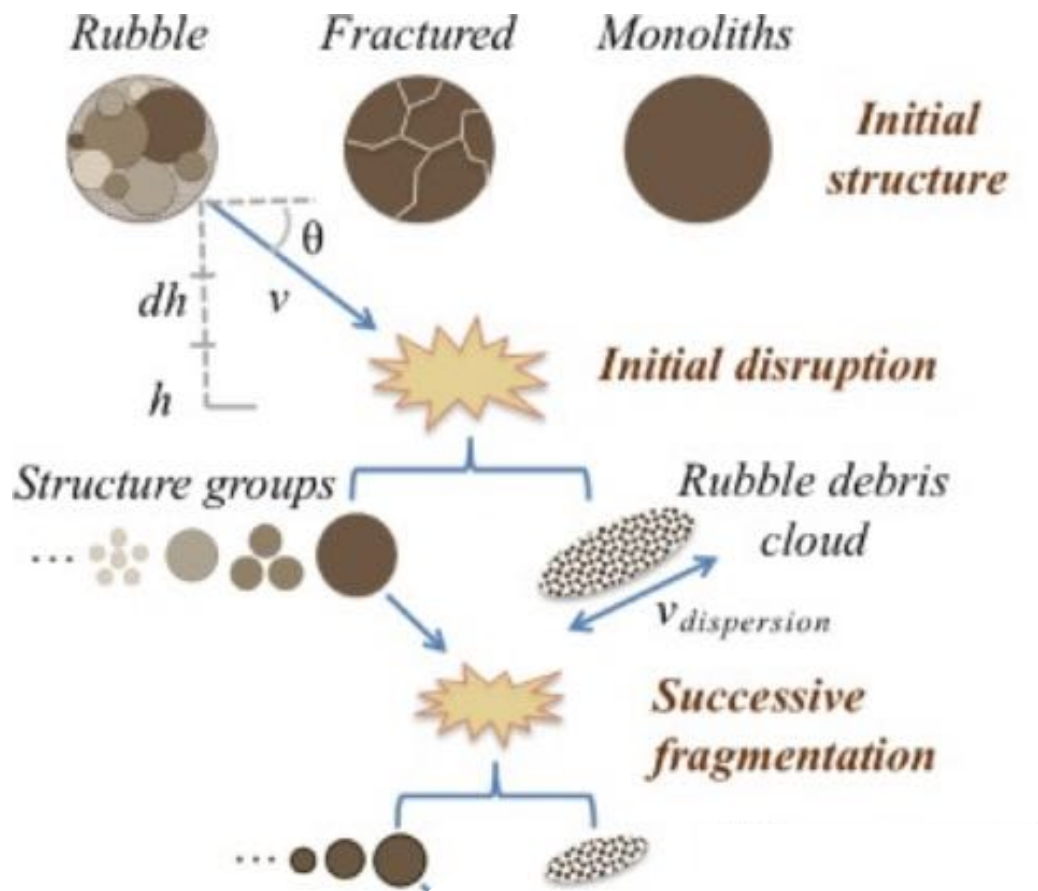
Strength scaling (α)



- Varied energy deposition curves represent uncertainties in breakup behavior and effective burst altitudes
- Inputs to high-fidelity blast simulations to assess specific entry cases

100 Mt, 120 m diameter, stony type asteroid, entering at 20 km/s and 45°

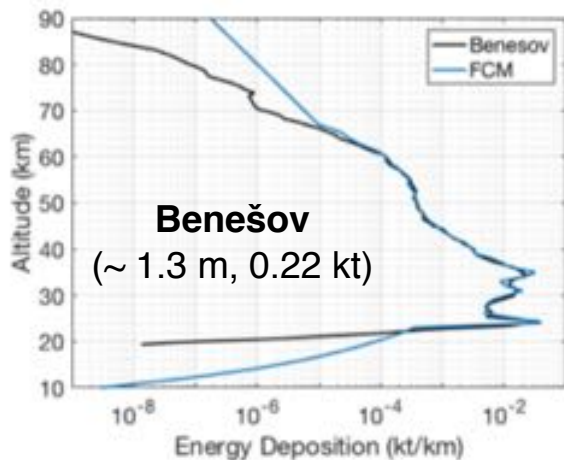
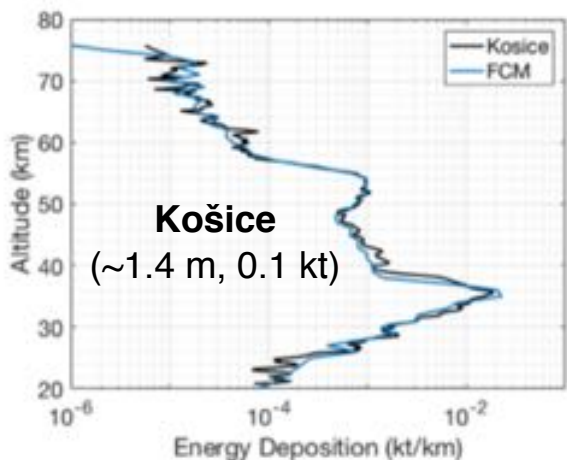
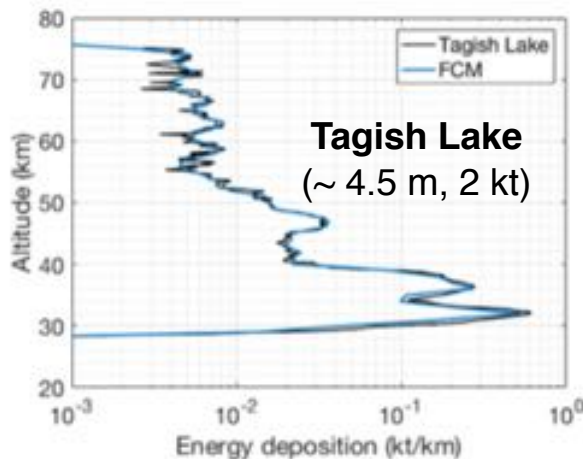
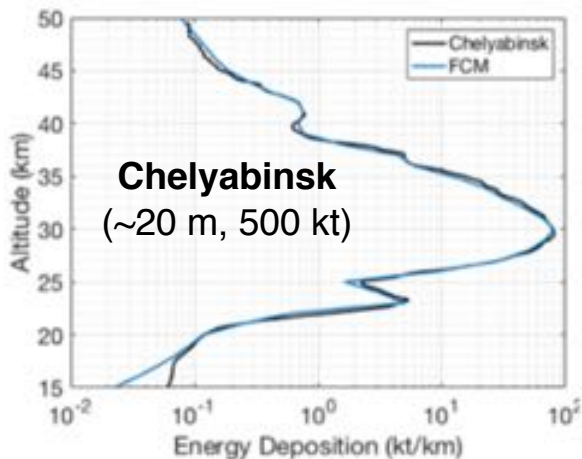
Varied Rubble Pile Structures in FCM



- Many asteroids have loose rubble pile compositions or significant fracturing
- Observed meteor entries exhibit a wide variety of flare features that cannot be reproduced by simpler uniform fragmentation models
- Added capability to represent these varied initial structures and breakup features

FCM Observed Meteor Modeling

- FCM with rubble pile structures enables matching of varied flare features for a range of observed meteor cases:

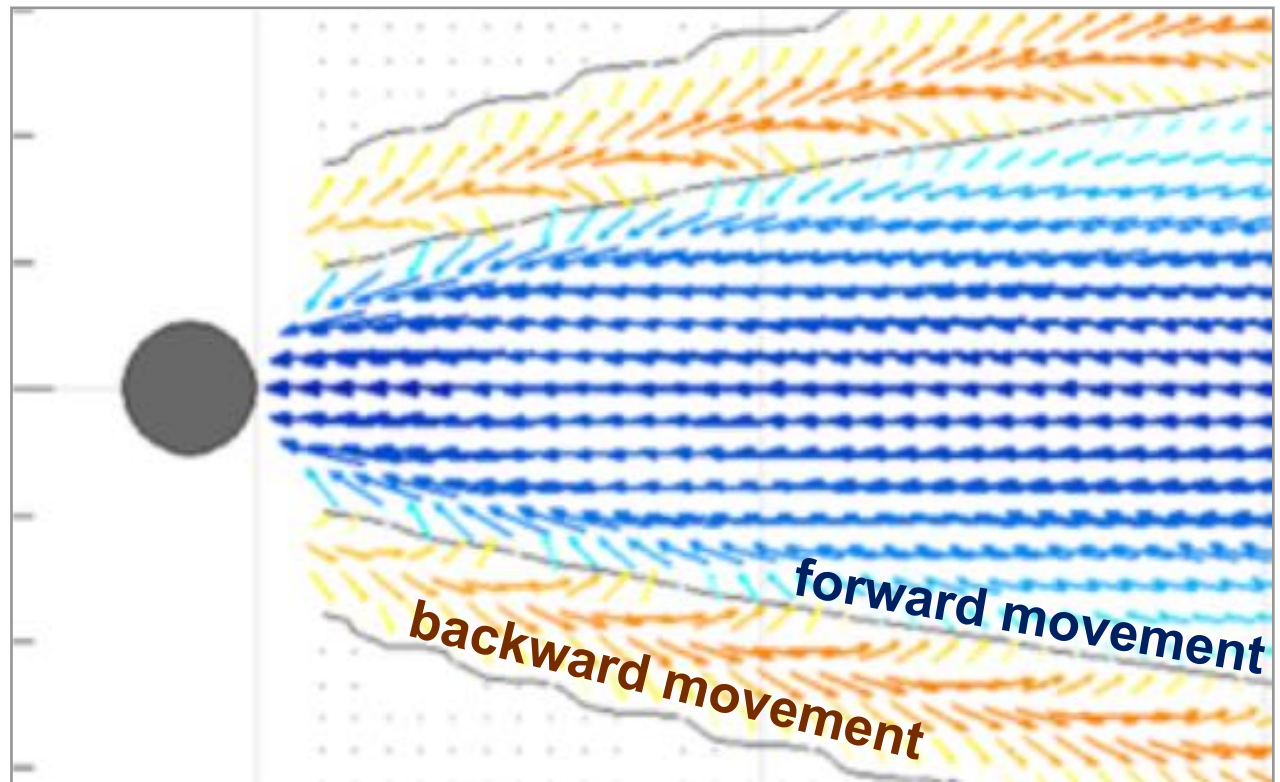
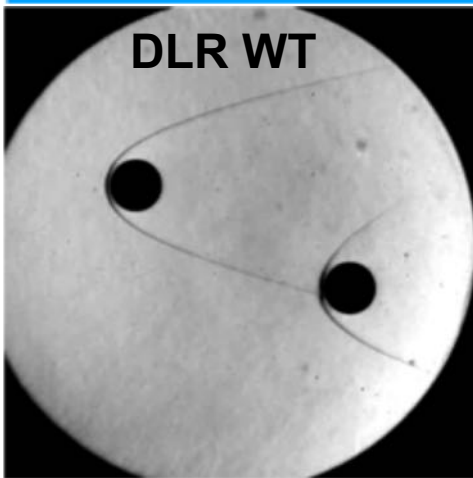
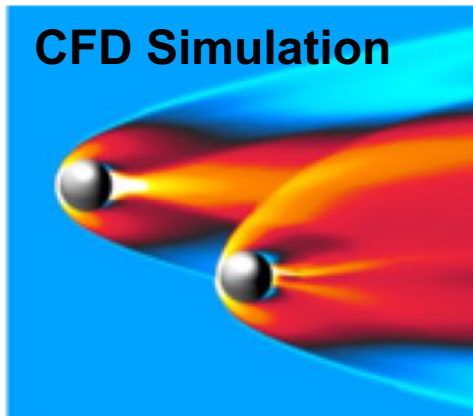


- Large flares best matched with moderately high debris cloud fractions (~80%) and moderate fragment strength scaling exponent (α).
- Lower ablation and debris cloud spread rates than baseline values.
- Variable ablation and luminous efficiency would improve matches and inferences capabilities across range of altitudes.

Meteor data from: Brown et al. (2013) and collaboration with P. Brown and E. Stokan.

Fragment Separation Model

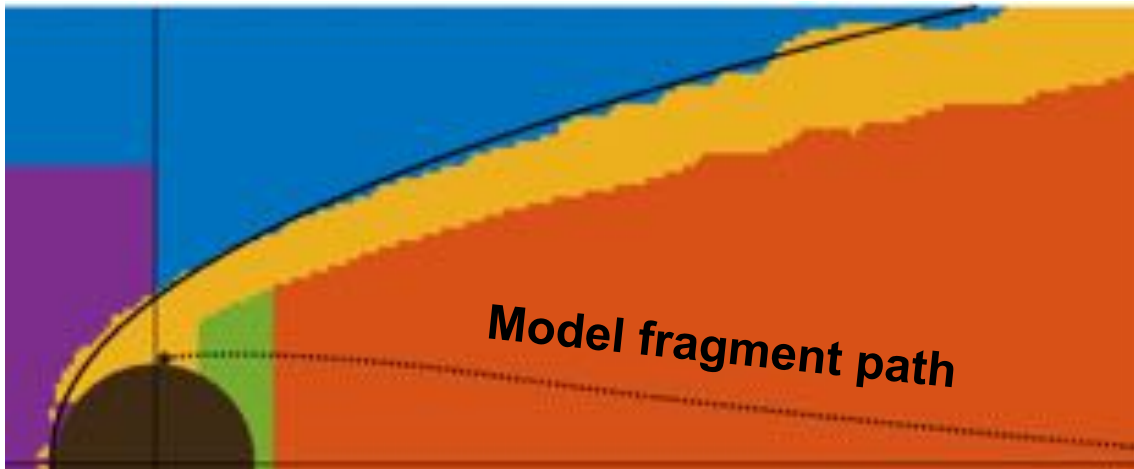
- Developing an analytic model of fragment separation due to wake interaction:
 - Based on database of force coefficients from multi-body CFD simulations
 - Validated with hypersonic wind tunnel experiments at DLR



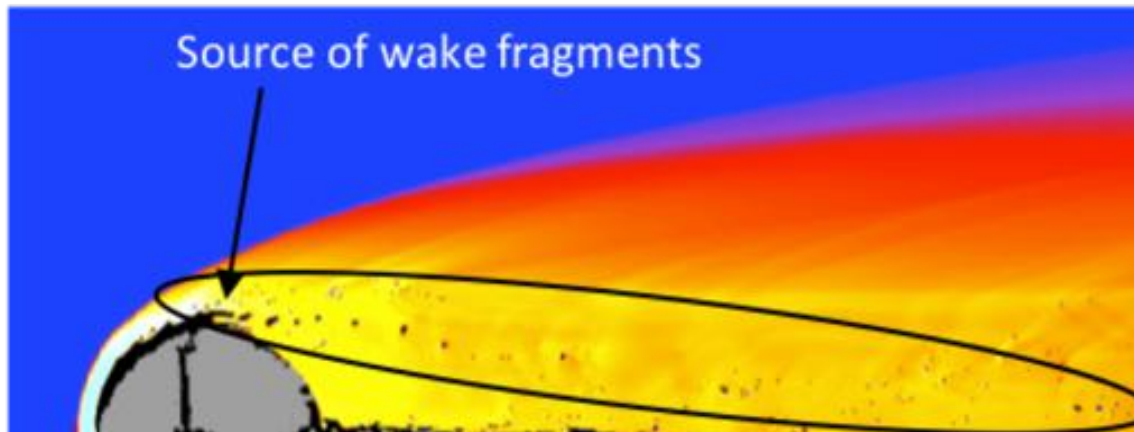
CFD force coefficients for relative motion of a second body due to wake interaction

Fragment Separation Model

- Model shows good agreement with CFD and hydrocode simulations.
- Also suggests slower spread rates than baseline pancake model values



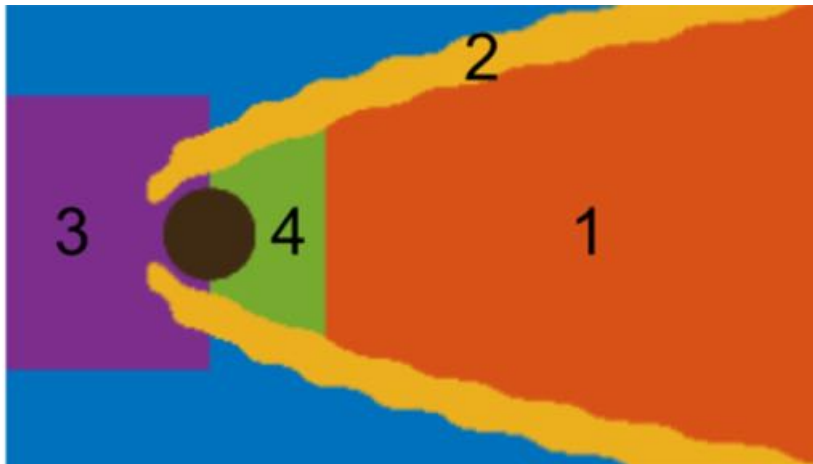
**Model-predicted
fragment path
through wake
zones**



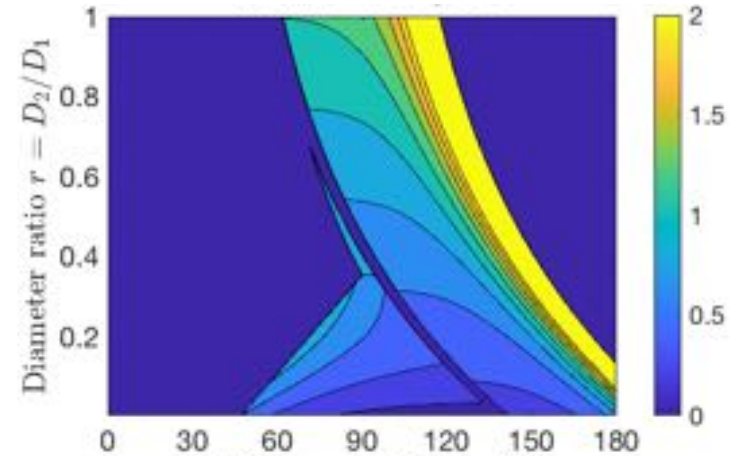
**ALE3D hydrocode
simulation**

Fragment Separation Model

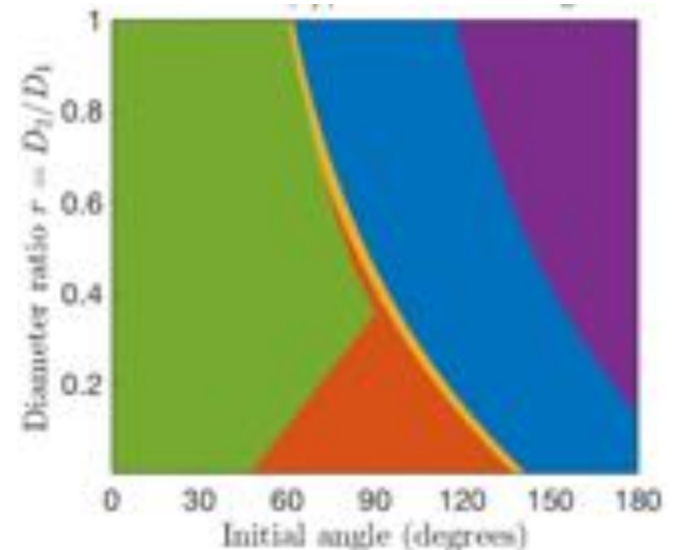
- Developed analytic model that gives final wake zones and separation times as a function of: relative fragment size and Initial position angle
- Will be used to replace the pancake spreading and instant fragment separation assumptions in FCM with more physically grounded mechanisms.

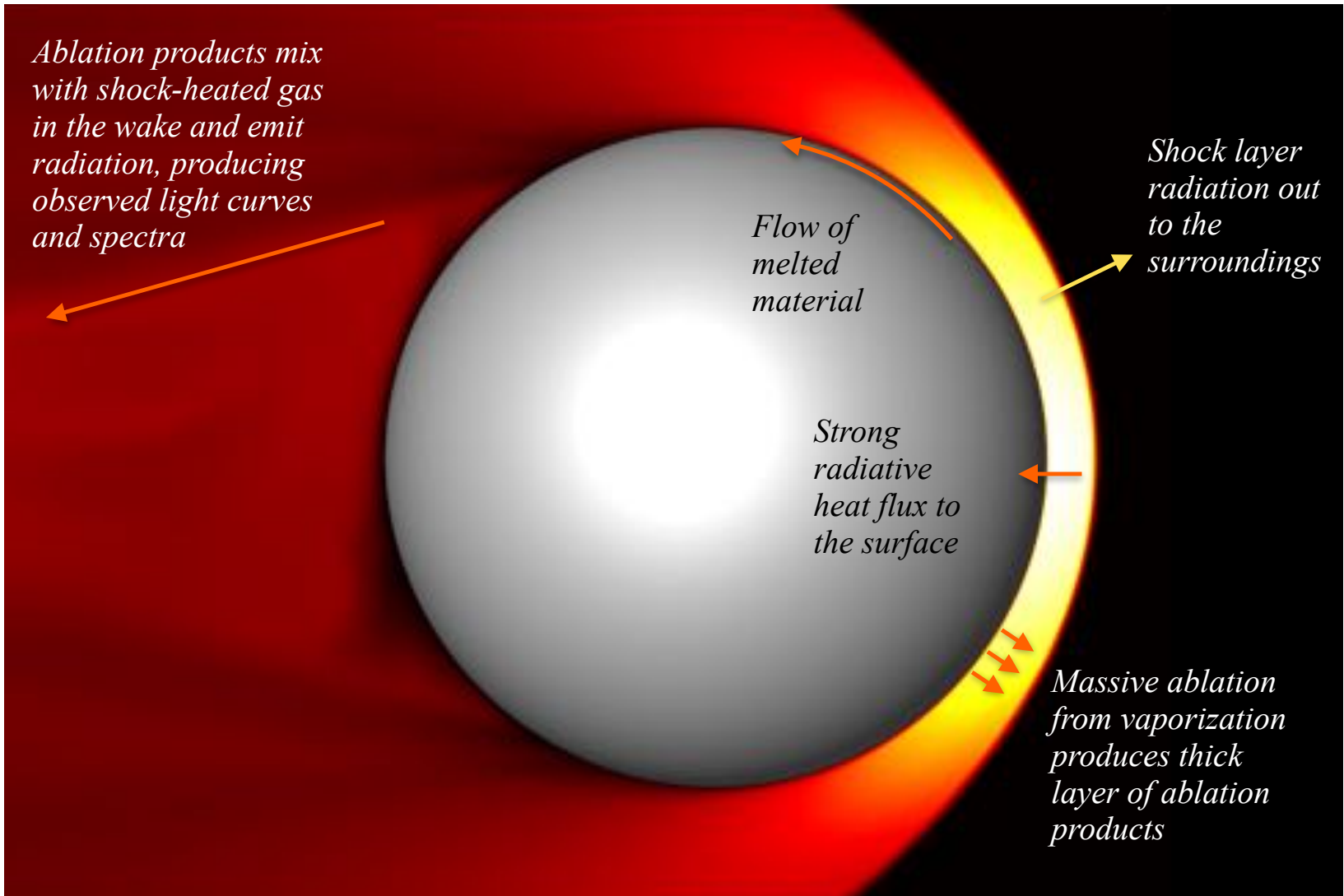


Time to Final Zone



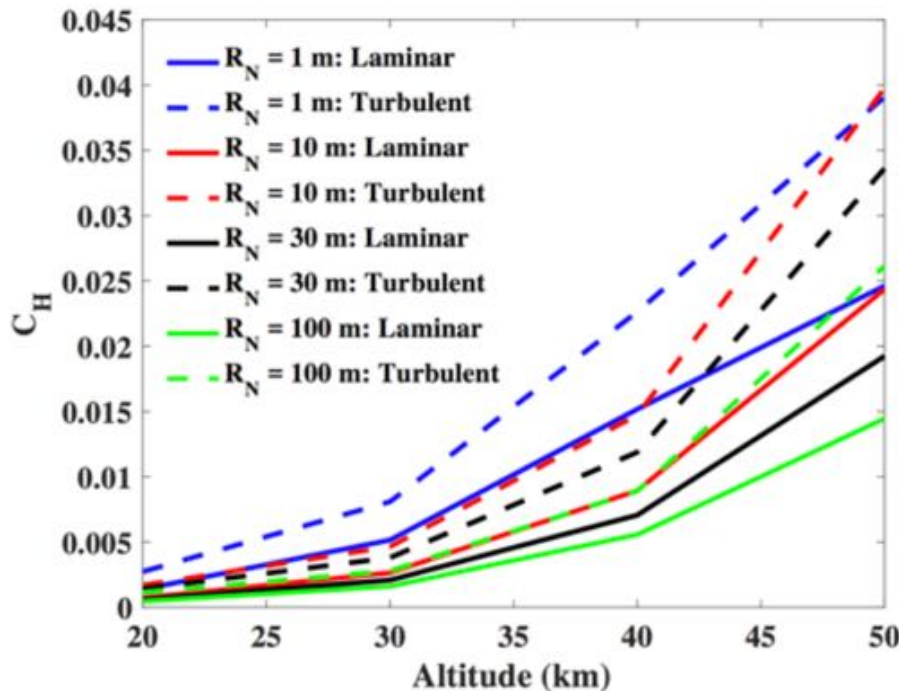
Final Wake Zones





Heat Transfer Modeling

- Chemically reacting computational fluid dynamics (CFD) simulations with coupled radiation transport and surface ablation.



- Curve fits of results provide an analytic model for variable heat transfer coefficient values (C_H) as a function of fragment velocity, altitude, and frontal radius
- Radiative cooling and radiation blockage reduce the effective C_H compared to heritage baseline value of 0.1

$$C_{H,Lam} = \frac{1.107 \times 10^{-3}}{V_{\infty} R_N^{0.22}} \exp(-8.5818 \times 10^{-4} h_{alt}^2 + 0.1753 h_{alt})$$

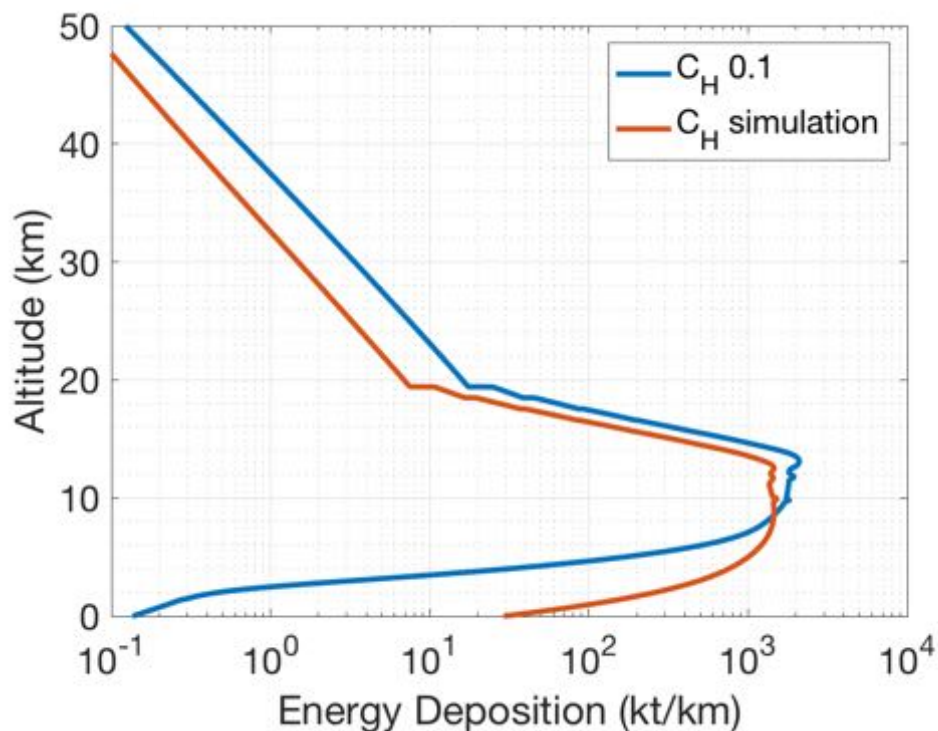
Single-body ablation

$$dm/dt = -0.5 \rho_{air} v^3 A \sigma$$

$$\sigma = C_H / Q_{ab}$$

Heat Transfer Modeling

- Effects of variable simulation-based C_H on FCM energy deposition:



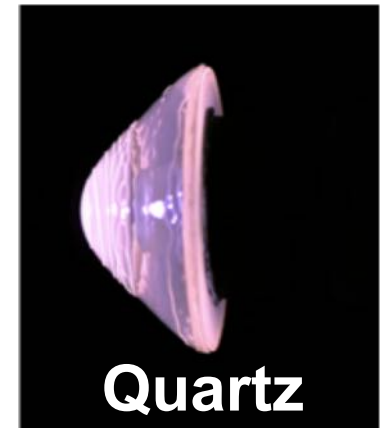
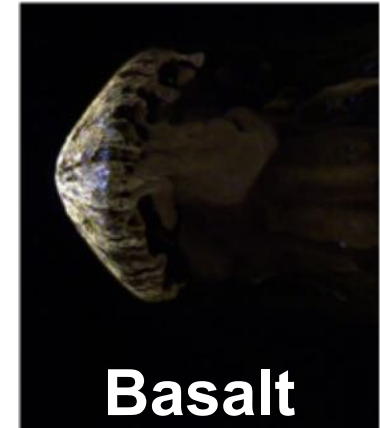
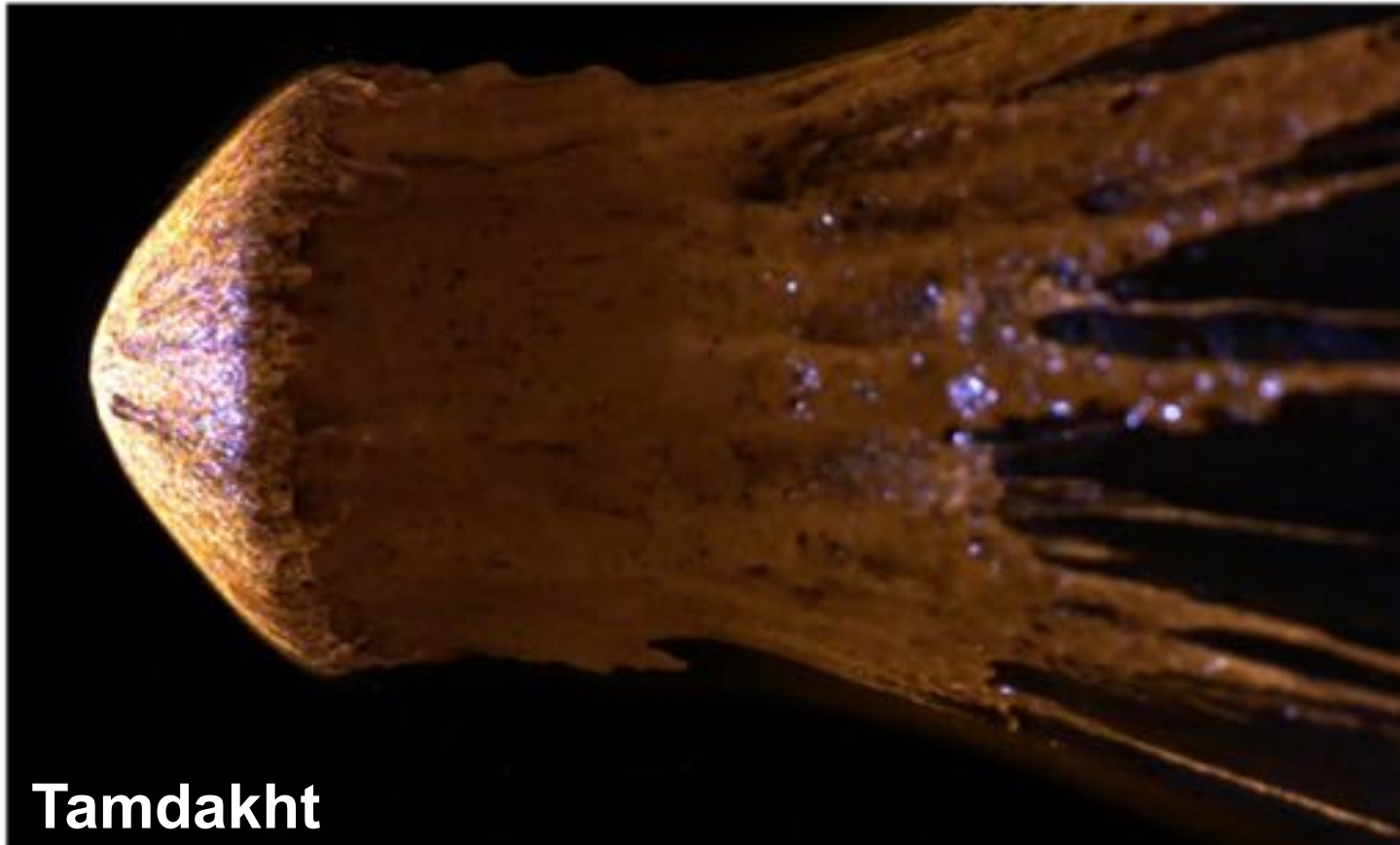
- Sample Tunguska-size case, vertical 20 km/s entry
- Lower ablation rates from simulation-based C_H
- Can lower burst altitude estimates by up to several kilometers for cases of this size range

$$C_{H,Lam} = \frac{1.107 \times 10^{-3}}{V_{\infty} R_N^{0.22}} \exp(-8.5818 \times 10^{-4} h_{alt}^2 + 0.1753 h_{alt})$$

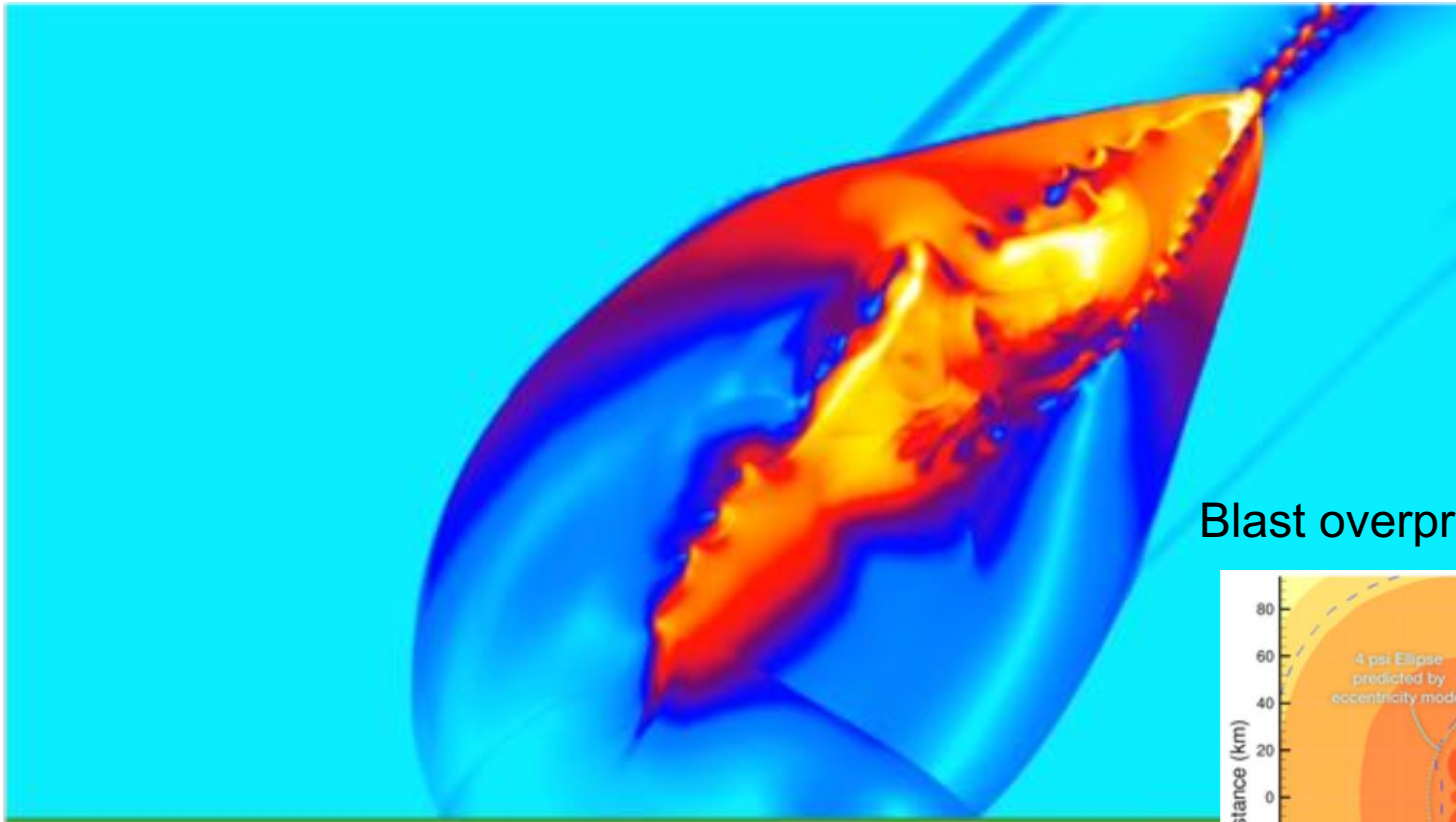
$$\begin{aligned} dm/dt &= -0.5 \rho_{air} v^3 A \sigma \\ \sigma &= C_H / Q_{ab} \end{aligned}$$

Arc Jet Ablation Experiments

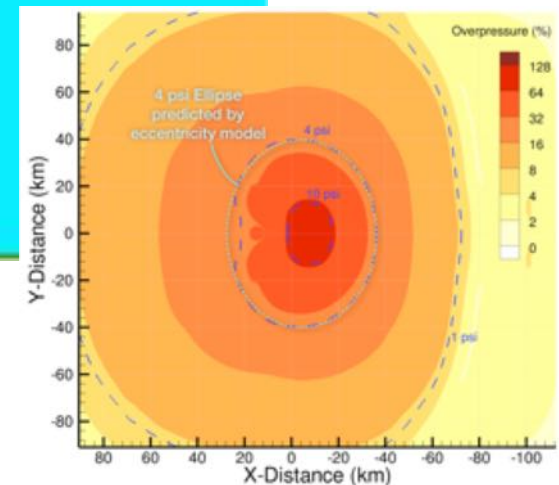
- Arc jet experiments to develop and validate improved models for meteoroid ablation and luminosity



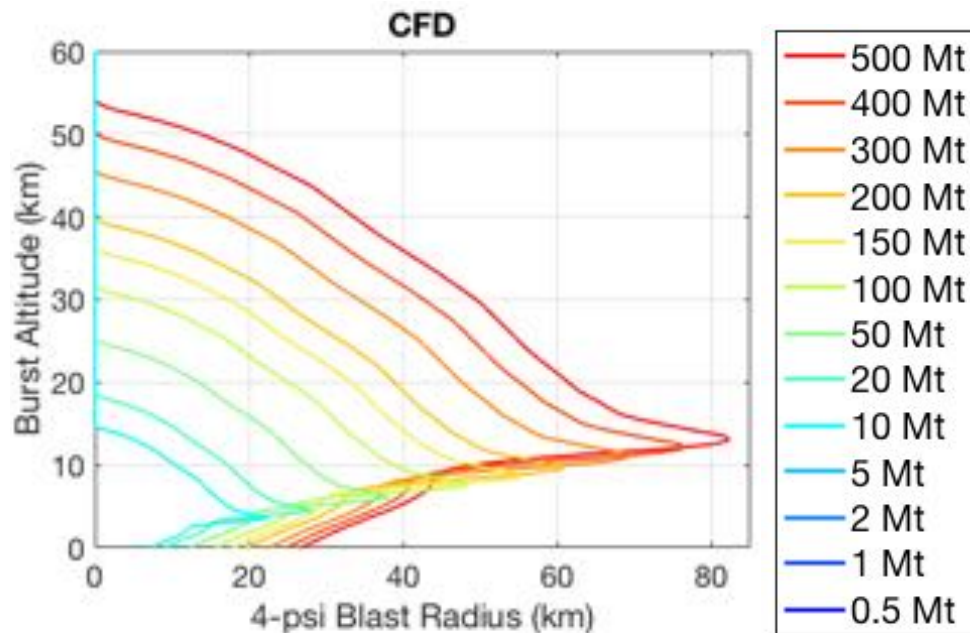
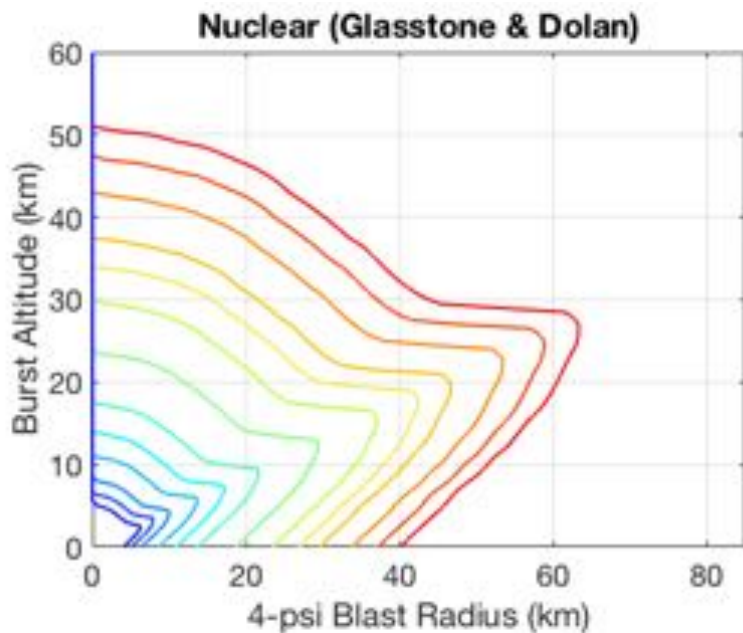
Cart3D computational fluid dynamics (CFD) blast propagation simulation



Blast overpressure footprint

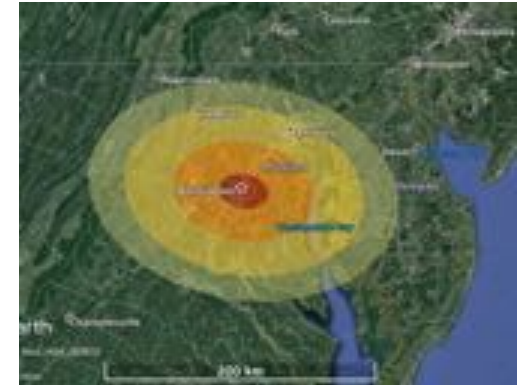


- HOB maps provide an efficient means of estimating blast overpressure ground radius as a function of effective burst altitude for a given energy (yield).
- Nuclear-based HOB maps are based on small yields (1 kt) that cannot be accurately scaled to large asteroid yields due to effects of buoyancy and longer time-scales
- Developed improved Height-of-Burst maps for large yields based on CFD blast simulations of 250 Mt airbursts.
- PAIR blast damage model now interpolates between nuclear curves for $E < 5$ Mt and simulation curves for $E > 250$ Mt

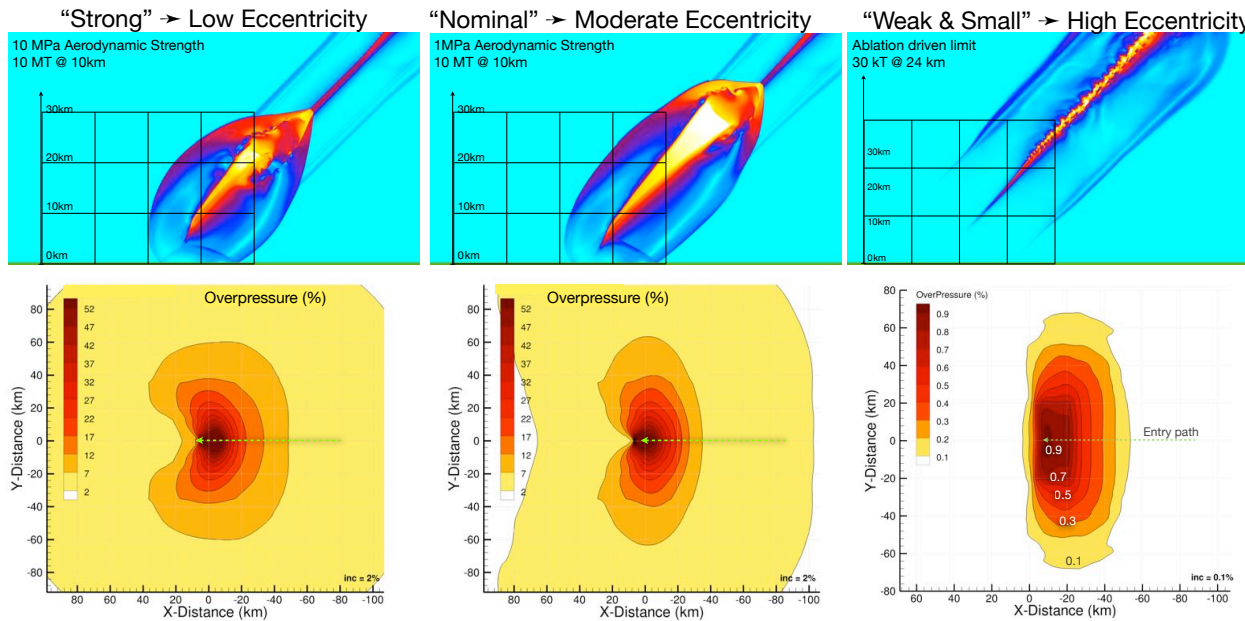


Blast Footprint Eccentricity

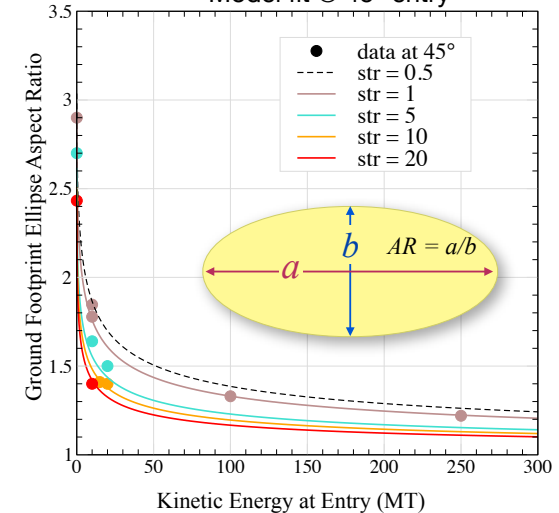
- Parametric model of blast footprint eccentricity based on CFD blast simulations.
- Estimates footprint aspect ratio as a function of entry angle, energy, and strength.
- Provides more accurate damage regions for risk assessment of location-specific impact scenarios



Simulation data @ 45° entry

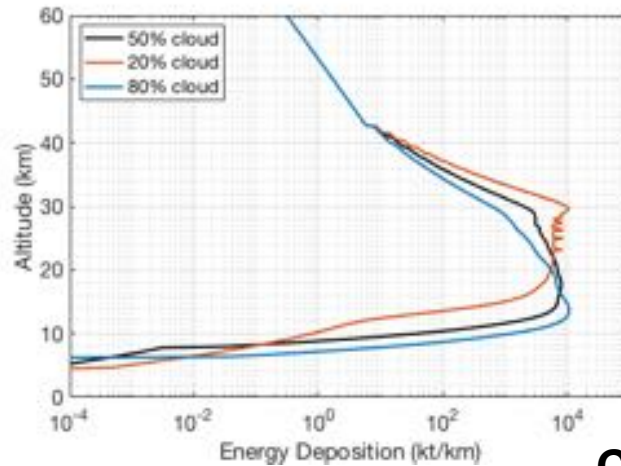


Model fit @ 45° entry



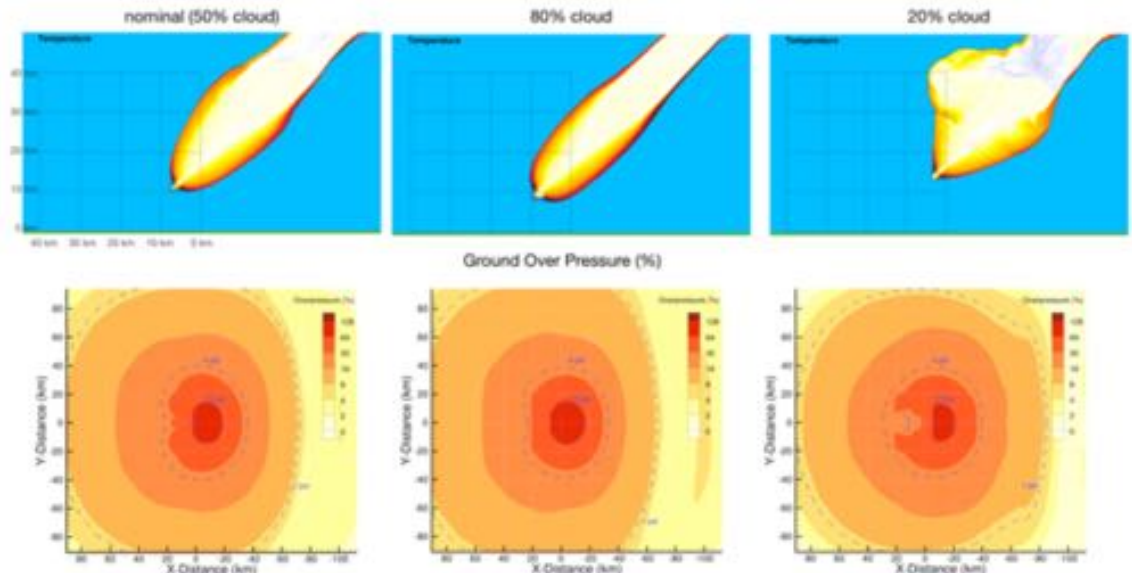
Parametric Energy Deposition Blast Footprint Modeling

- Working toward developing parametric ground footprints based on CFD blast simulations initiated with varied FCM energy deposition curves
- Replace static point-source model based on effective height-of-burst
- Capture effects of varied breakup rates and features on ground footprints

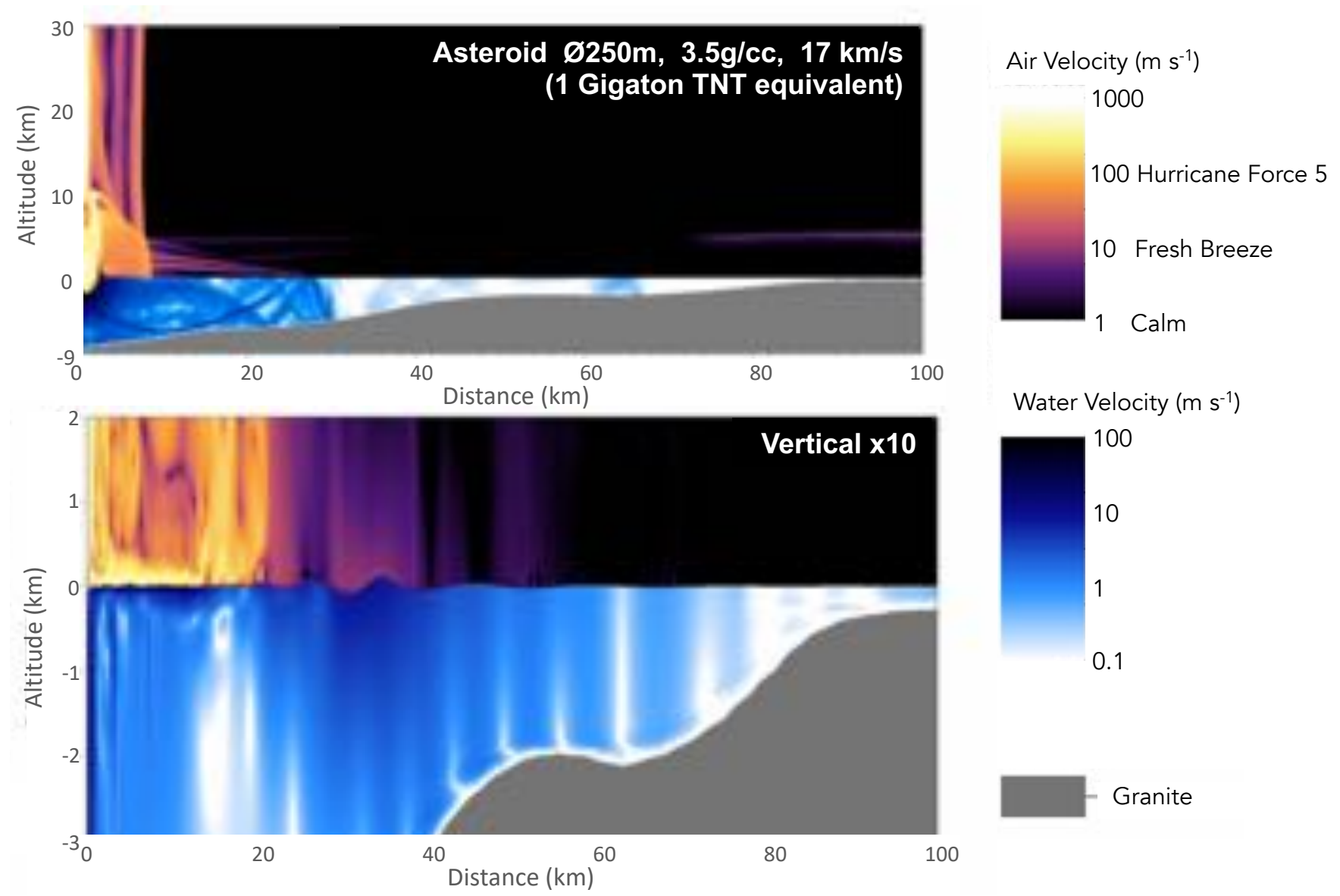


Energy deposition variations

CFD blast propagation

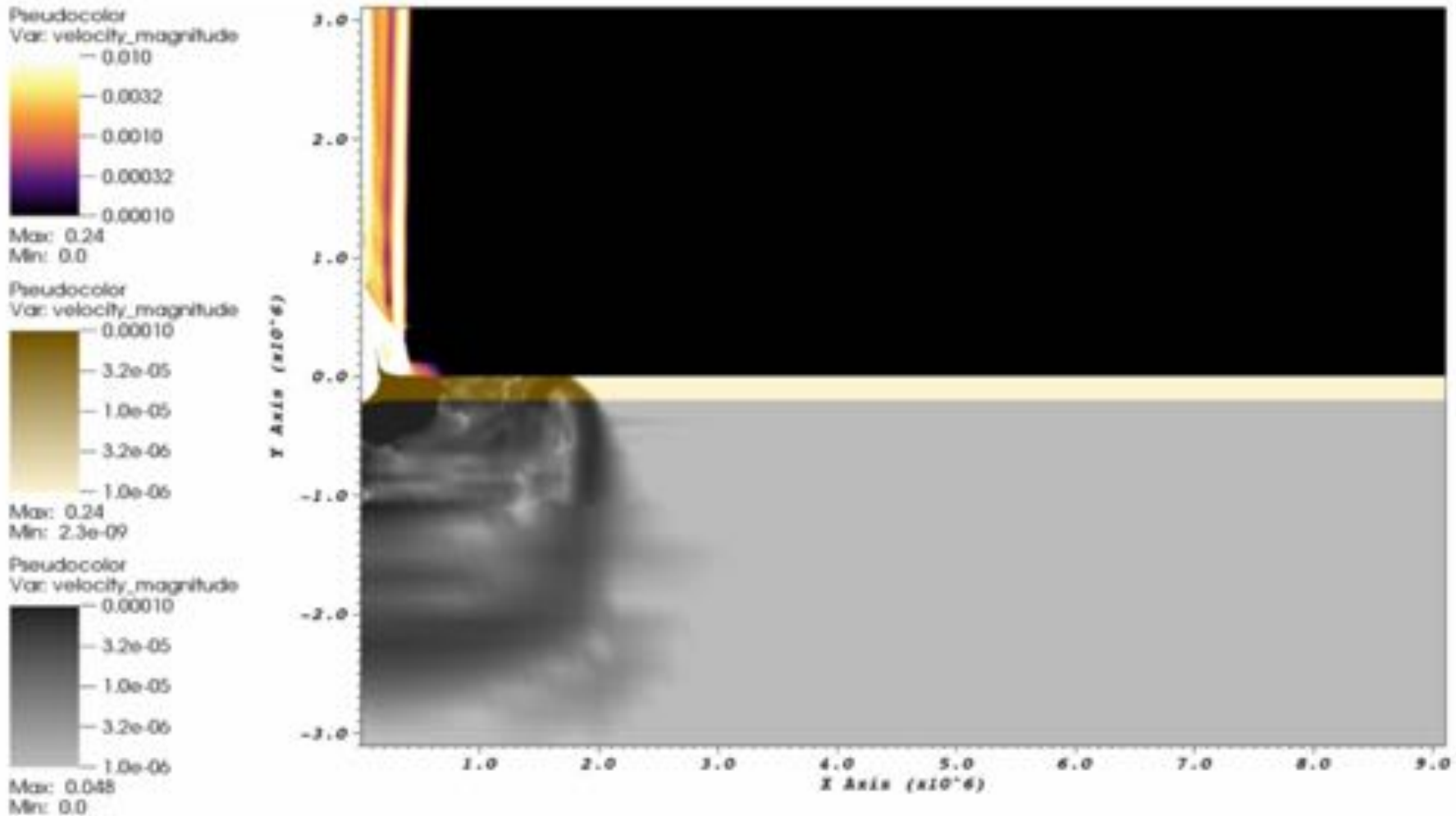


ALE3D Hydrocode Tsunami Simulations



ALE3D Land Impact Simulation

Asteroid $\varnothing 250\text{m}$, 3.5g/cc , 17 km/s
(1 Gigaton TNT equivalent)



ATAP Team Contributors

Characterization

- Jessie Dotson
- Daniel Ostrowski
- Diane Wooden

Observations

- Randy Longenbaugh
- Christopher Henze

Entry Simulations & Testing

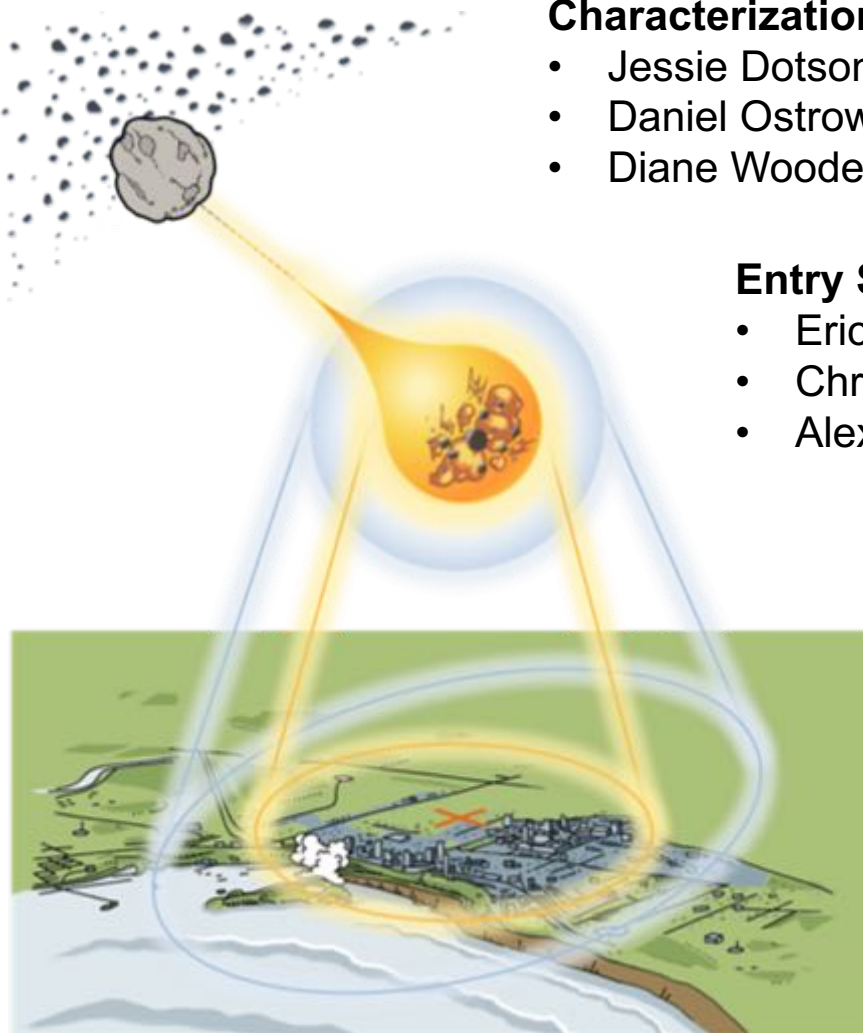
- Eric Stern
- Christopher Johnston
- Alex Zibitsker
- Parule Agrawal
- Justin Haskins
- Charles Bauschlicher
- John Lawson

Hazard Simulations & Modeling

- Michael Aftosmis
- Darrel Robertson
- Marian Nemec
- Wade Spurlock
- Marsha Berge
- Randall LeVeque

Probabilistic Risk Modeling:

- Donovan Mathias
- Lorien Wheeler
- Clemens Rumpf
- Paul Register
- Ana Tarano



Probabilistic Risk Assessment

- Mathias, D.L., Wheeler, L.F., Dotson J.L., 2017. A probabilistic asteroid impact risk model: assessment of sub-300m impacts. *Icarus* 289, 106–119. <https://doi.org/10.1016/j.icarus.2017.02.009>
- Wheeler, L.F., Mathias, D.L., 2019. Probabilistic assessment of Tunguska-scale asteroid impacts. *Icarus*, 327, 83–96. <https://doi.org/10.1016/j.icarus.2018.12.017>
- Wheeler, L.F., Mathias, D.L., 2019. Effects of asteroid property distributions on expected impact rates. *Icarus* 321, 767–777. <https://doi.org/10.1016/j.icarus.2018.12.034>

FCM

- Wheeler, L.F., Mathias, D.L., Stokan, E., Brown, P.G., 2018. Atmospheric energy deposition modeling and inference for varied meteoroid structures. *Icarus* 315, 79–91. <https://doi.org/10.1016/j.icarus.2018.06.014>
- Wheeler, L.F., Register, P.J., Mathias, D.L., 2017. A fragment-cloud model for asteroid breakup and atmospheric energy deposition. *Icarus* 295, 149–169. <https://doi.org/10.1016/j.icarus.2017.02.011>
- Register, P. J., Mathias, D.L., Wheeler, L.F., 2017. Asteroid fragmentation approaches for modeling atmospheric energy deposition. *Icarus* 284C, 157–166. <https://doi.org/10.1016/j.icarus.2016.11.020>
- Tarano, A.M., Mathias, D., Wheeler, L., Close, S., 2019. Inference of Meteoroid Characteristics Using a Genetic Algorithm. *Icarus*, in press, accepted 3 April, 2019.

Hazard Simulations

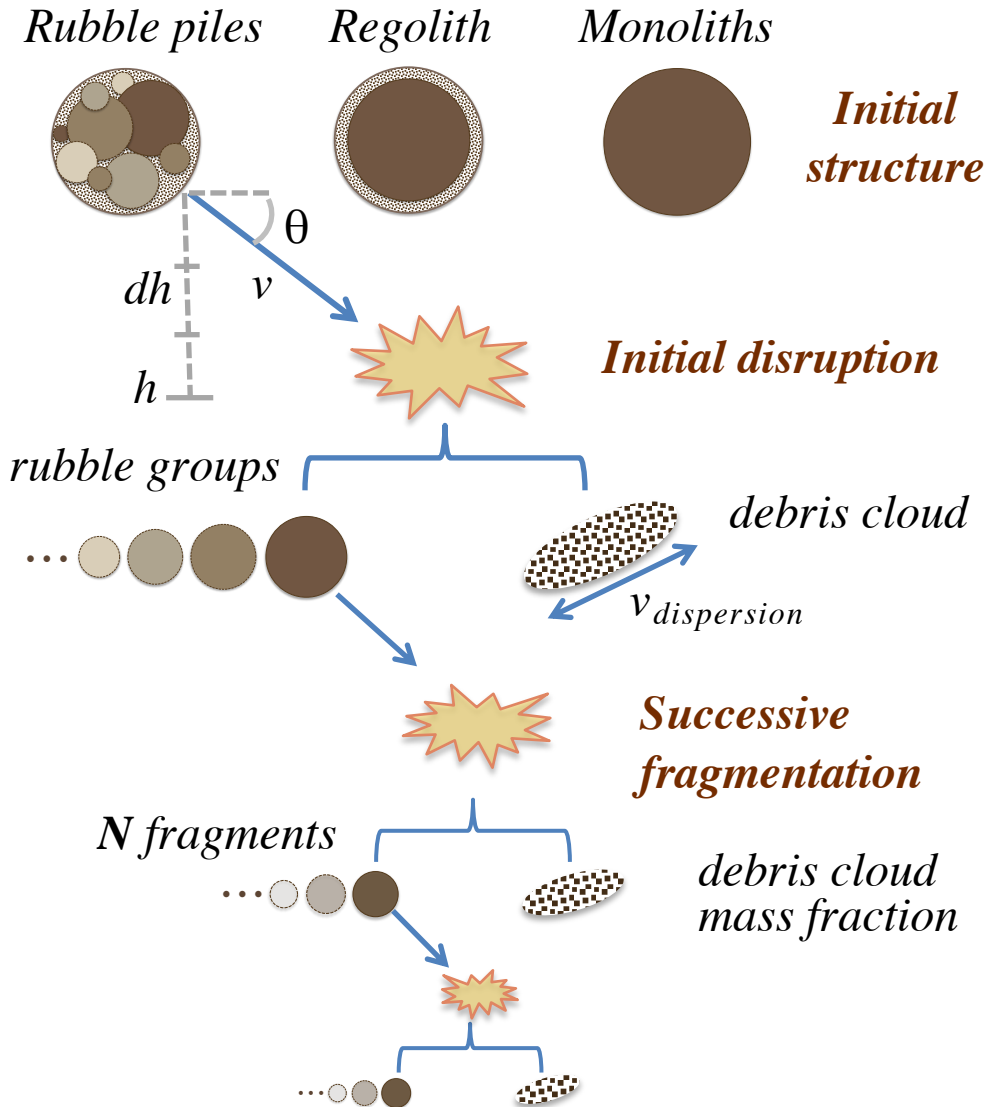
- Aftosmis, M.J., Mathias, D.L., Tarano, A.M., 2017. Simulation-based height of burst map for asteroid airburst damage prediction. *Acta Astronautica*, In Press. <https://doi.org/10.1016/j.actaastro.2017.12.021>
- Aftosmis, M.J., Nemec, M., Mathias, D., Berger, M., 2016. Numerical simulation of bolide entry with ground footprint prediction. 54th AIAA Aerospace Sciences Meeting, AIAA SciTech Forum, (AIAA 2016-0998). <https://doi.org/10.2514/6.2016-0998>
- Robertson, D.K., Mathias, D.L., 2019. Hydrocode simulations of asteroid airbursts and constraints for Tunguska. *Icarus*, 327. <https://doi.org/10.1016/j.icarus.2018.10.017>
- Robertson, D. K., Mathias, D.L., 2017. Effect of yield curves and porous crush on hydrocode simulations of asteroid airburst. *J. Geophys. Res. Planets*, 122, 599–613. <https://doi.org/10.1002/2016JE005194>
- Robertson, D.K., Gisler, G.R., 2018. Near and far-field hazards of asteroid impacts in oceans. *Acta Astronautica*, in press, available online 18 Sept. 2018. <https://doi.org/10.1016/j.actaastro.2018.09.018>

Entry Physics

- Johnston, C.O., Stern, E.C., 2018. A model for thermal radiation from the Tunguska airburst. *Icarus*, in press, submitted 24 July 2018.
- Johnston, C.O., Stern, E.C., Wheeler, L.F., 2018. Radiative heating of large meteoroids during atmospheric entry. *Icarus* 309, 25–44. <https://doi.org/10.1016/j.icarus.2018.02.026>
- Haskins, J. B., Stern, E.C., Bauschlicher, C. W., Lawson, J. W., 2019. Thermodynamic and Transport Properties of Meteor Melt Constituents from Ab Initio Simulations: MgSiO₃, SiO₂, and MgO. *Journal of Applied Physics*, in press.

BACKUP

Fragment-Cloud Model (FCM)



Flight integration:

$$dm/dt = -0.5 \rho_{air} v^3 A \sigma$$

$$dv/dt = \rho_{air} v^2 A C_D / m - g \sin \theta$$

$$d\theta/dt = (v / (R_E + h) - g / v) \cos \theta$$

$$dh/dt = v \sin \theta$$

Fragmentation condition:

$$\rho_{air} v^2 > \text{Strength } (S)$$

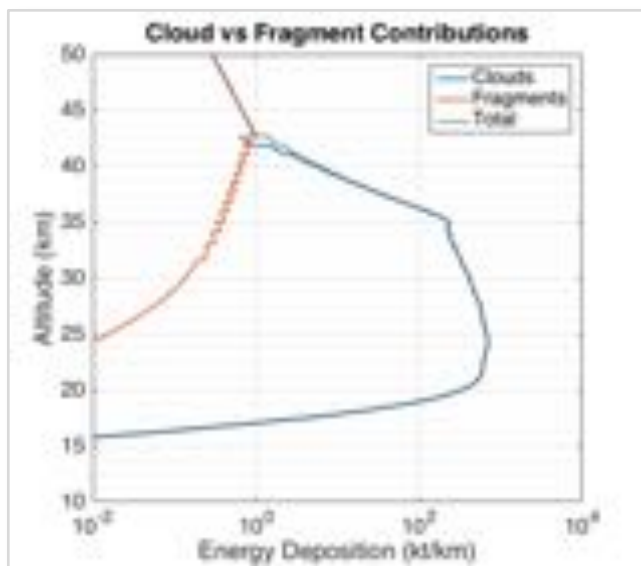
Fragment strengths increase with decreased size

$$S_{child} = S_{parent} (m_{parent} / m_{child})^\alpha$$

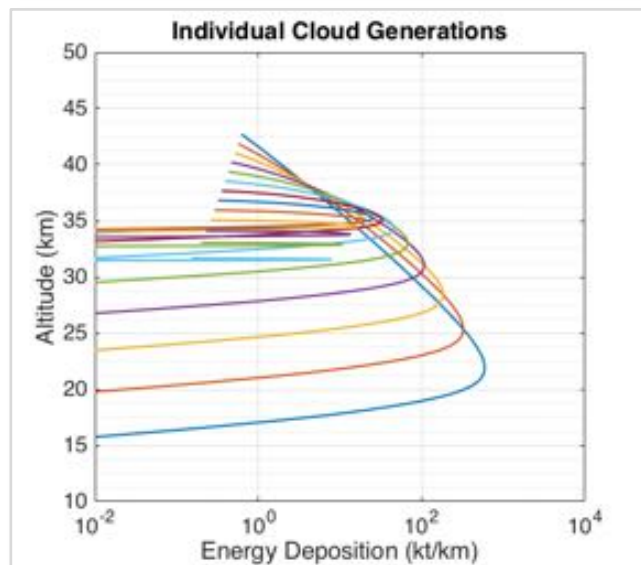
Clouds broaden and slow under common bow shock

$$v_{disp.} = v_{cloud} (C_{disp} A \rho_{air} / \rho_{debris})^{1/2}$$

FCM Energy Deposition

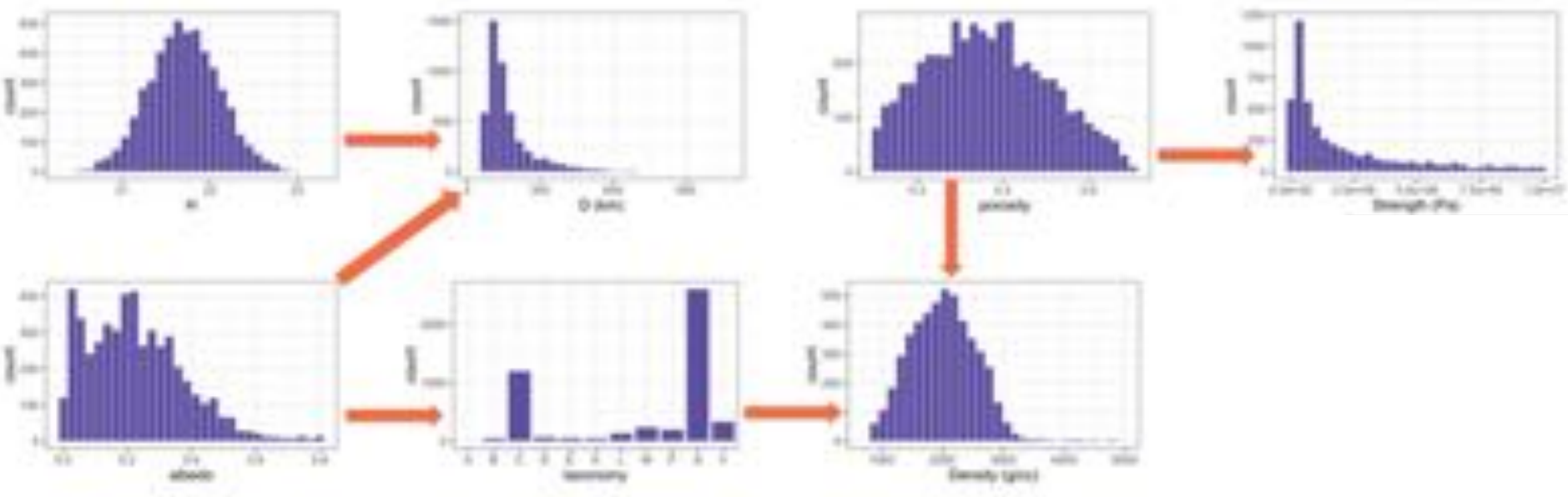


- Energy deposited in the atmosphere as a function of altitude (kt/km)
- Variable energy deposition mechanisms:
 - Debris clouds deposit the bulk of the energy as they rapidly spread, slow, and
 - Fragments serve to distribute the release of varied cloud masses
 - Large debris clouds released higher up produce broad, gradual flares
 - Small clouds released lower down produce sharper peaks



Asteroid Property Inference Network

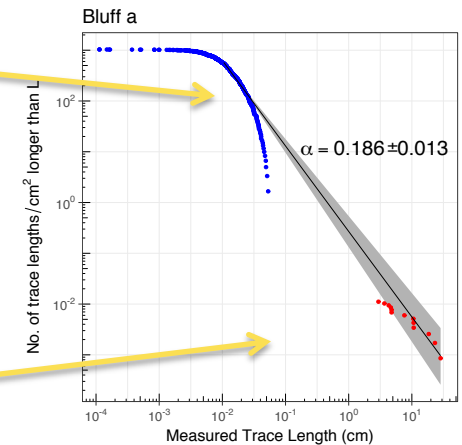
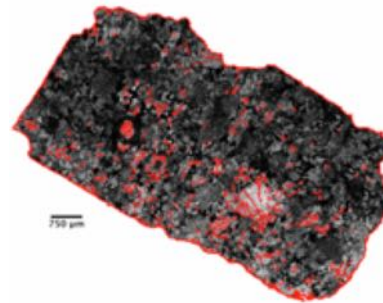
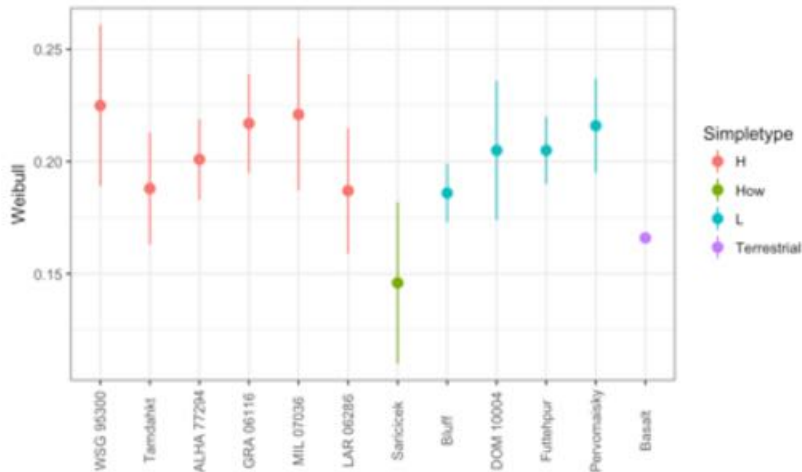
- A network to infer the asteroid properties required for probabilistic risk assessment was prototyped and exercised for the PDC 2019 exercise.
- The network is based on available measurements of the distribution of properties, but links the inferred properties in order to be physically consistent.
- The network below illustrates the linkages between distributions used to simulate asteroids for the first day of the PDC 2019 scenario.



Meteorites as Asteroid Samples

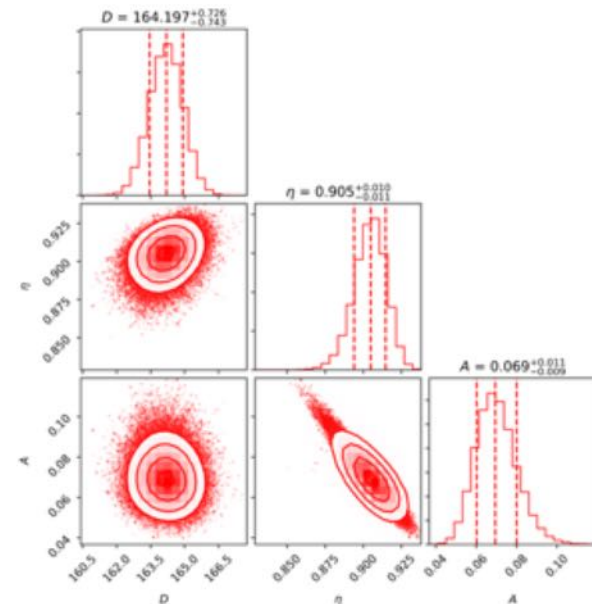
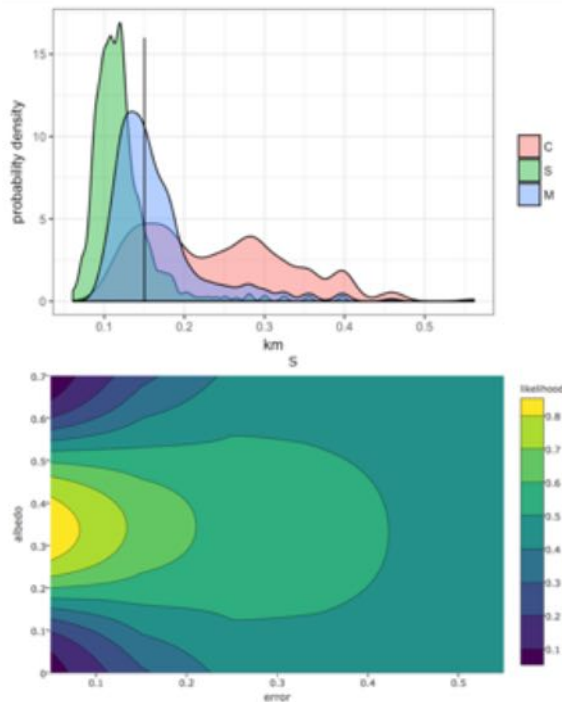
- Measuring physical properties of a variety of meteorite types:
 - Bulk density
 - Grain density
 - Thermal emissivity
 - Acoustic velocity

- Weibull scaling parameter (α) from visually observed fracture patterns.
 - Based on measured length and density of seams
 - α can be used in entry models to describe fracturing behavior in FCM
 - $S_{child} = S_{parent}(m_{parent}/m_{child})^\alpha$

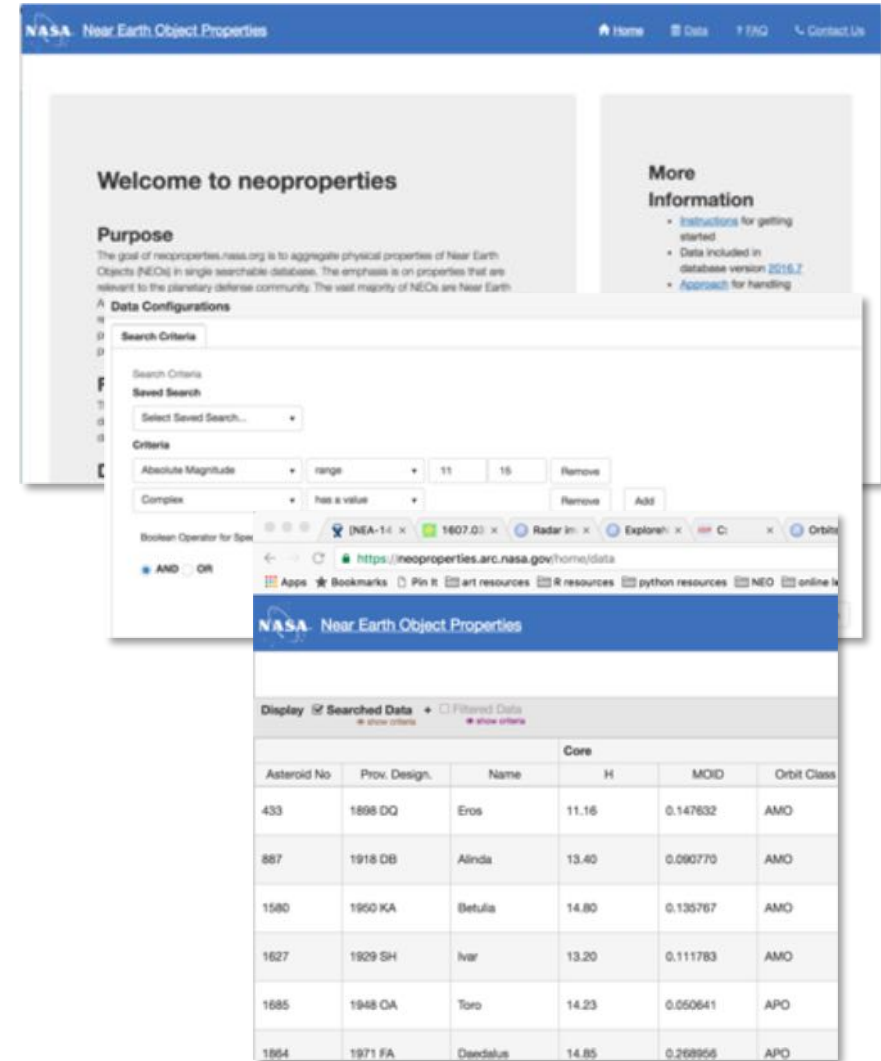


Asteroid Characteristics

- Inferring characteristics and distributions
 - Developed distributions of key asteroid characteristics for use in risk models
 - Developing methodology to quantitatively infer characteristics given limited information.
- Thermal modeling of IR observations to infer size & albedo
 - ATAP is combining standard heuristic models (NEATM, NESTM) modern algorithms (e.g. MCMC) .
 - Size is a *key* quantity to understanding potential damage.
 - Albedo provides hints of composition.



- neoproperties website
 - Aggregates physical properties of NEOs and meteorites into a searchable database
 - Emphasis on properties of interest to the planetary defense community
- Asteroid contents include:
 - Taxonomic class
 - Diameters & albedos
- Meteorite contents include:
 - Density & porosity
 - Compressive & tensile strength
 - Elastic & shear moduli
 - Heat capacity & thermal conductivity
- Includes a mapping between asteroids and similar meteorites

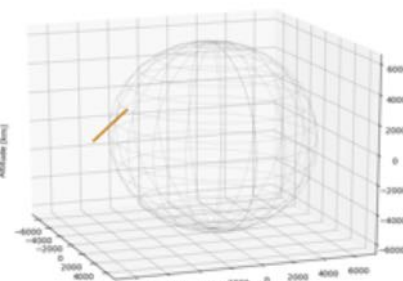
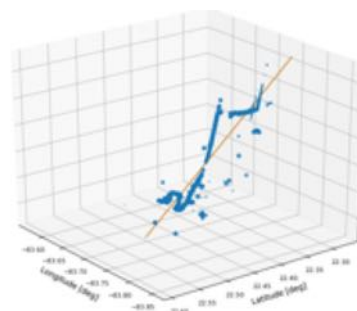
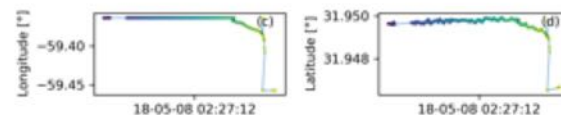
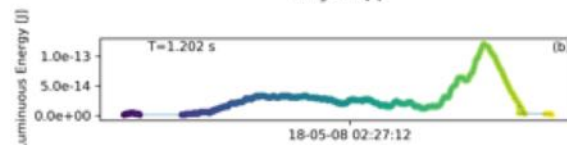
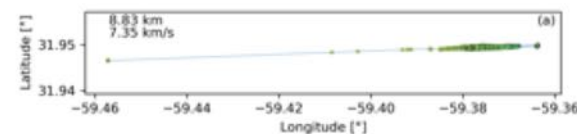
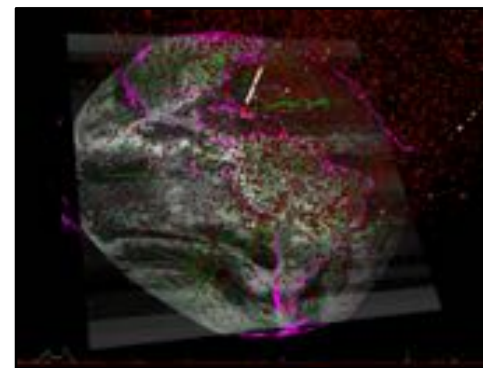


The screenshot shows the NASA Near Earth Object Properties website. The page includes a search interface with a 'Search Criteria' section where users can define search parameters. Below the search interface, a table displays a list of asteroids with their physical and orbital properties.

Core					
Asteroid No.	Prov. Design.	Name	H	MOID	Orbit Class
433	1898 DQ	Eros	11.16	0.147632	AMO
887	1918 DB	Alinda	13.40	0.090770	AMO
1580	1960 KA	Betulia	14.80	0.135767	AMO
1627	1929 SH	Ivar	13.20	0.111783	AMO
1685	1948 OA	Toro	14.23	0.050641	APO
1864	1971 FA	Daedalus	14.85	0.268956	APO

Bolide Detection with GLM

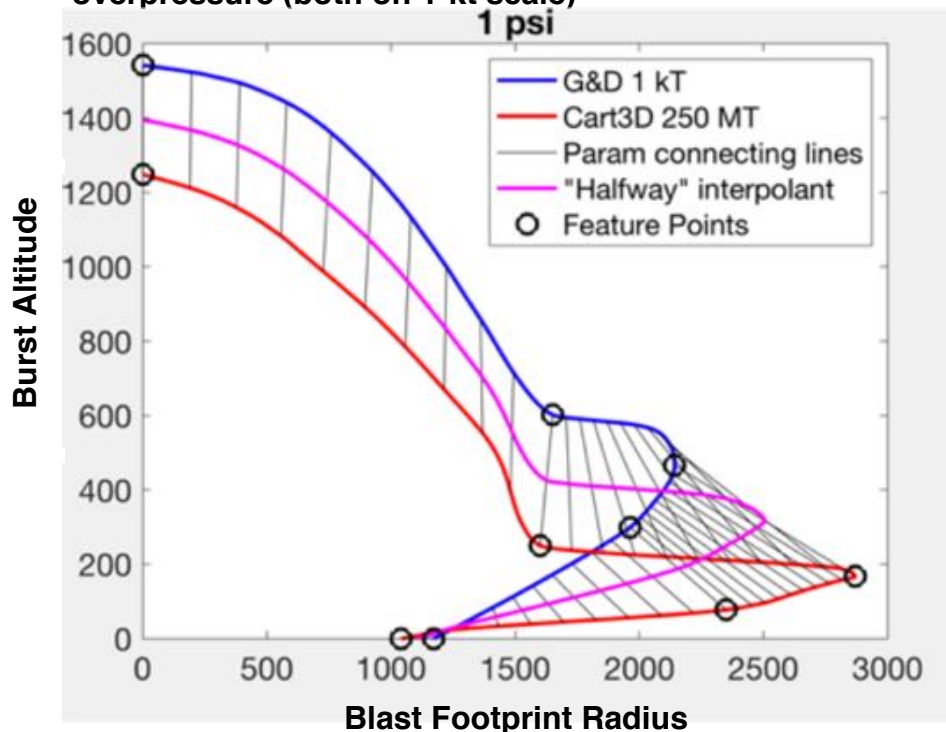
- Meteors are observable with the Geostationary Lightning Mapper (GLM) instrument on two NOAA satellites (GOES 16 & 17).
- A prototype detection pipeline is in place that identifies meteor signatures in GLM data.
- Current detection rate is
 - about 4 meteors per week
 - About 2 stereo detections per week
- Stereo detections enable 3D reconstruction of trajectory
- Future objectives:
 - Publish meteor detections
 - Publish trajectories, source energies
 - Build database on meteor influx
 - Infer meteor properties from light curves



Blast Footprint Modeling

- Height-of-Burst (HOB) maps provide efficient estimate blast footprint radii for as a function of burst altitude for a given energy
 - Estimates are typically yield-scaled from HOB maps for smaller nuclear sources (1-kt maps from Glasstone & Dolan).
 - This becomes inaccurate for larger yields due to buoyancy effects
- Developed improved Height-of-Burst maps for large yields based on CFD blast simulations (250 Mt).
- PAIR risk model uses
 - Nuclear curves for yields <5 Mt
 - Simulation curves for >250 Mt
 - Interpolates between them for intermediate energies

Feature-mapped interpolation between nuclear G&D and Cart3D simulation HOB curves for 1-psi blast overpressure (both on 1-kt scale)

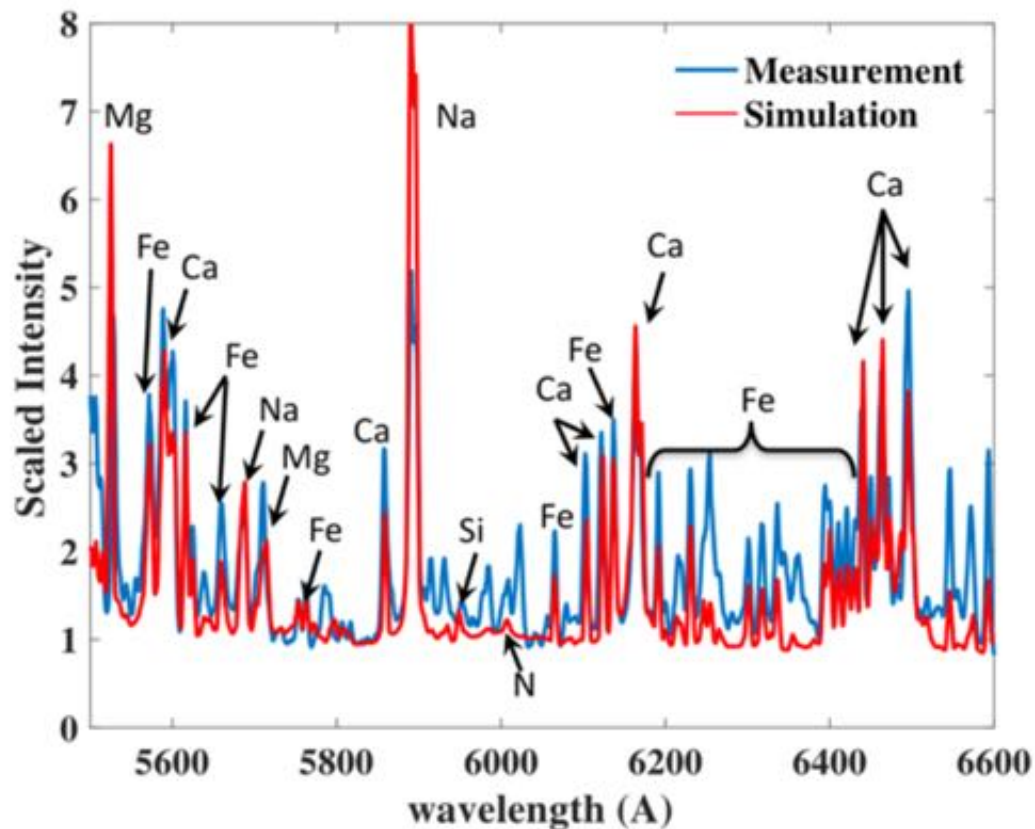


Simulated Emission Spectra



Measurement from Borovicka et al.

- The Benesov bolide from the Czech Republic provided one of the best spectra for a large meteor event
- Simulations of the Benesov meteoroid have been performed at several altitudes, and the emission spectrum to an observer on the ground computed
- Preliminary comparisons to data from the event show very promising agreement in terms of composition and relative line intensities

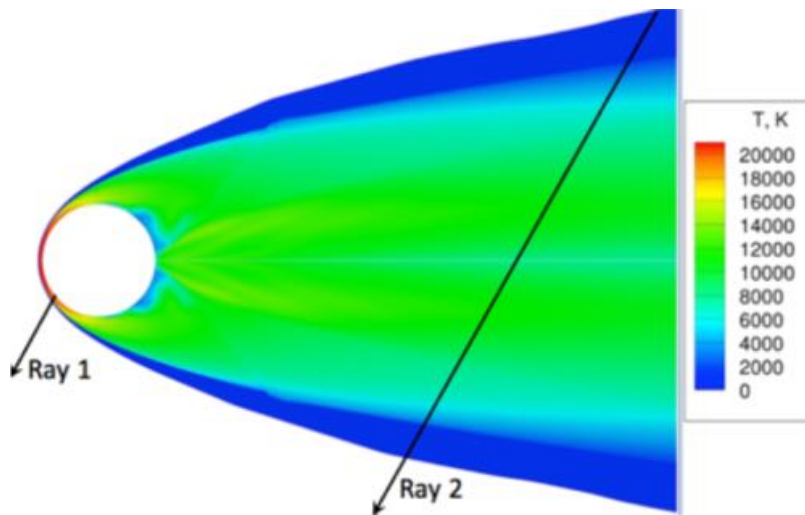


Luminous efficiency has been, and remains, a *highly* uncertain (yet important) parameter in meteor physics

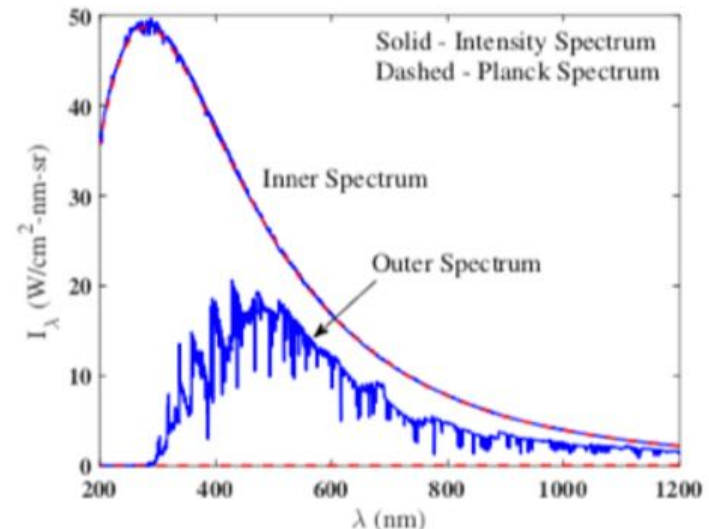
Tunguska Thermal Radiation

A model for airburst thermal radiation has been developed using the high-fidelity coupled approach previously used for meteoroid heat transfer

- Most thermal radiative flux at the ground originates from near-wake region, giving rise to strong viewing angle dependence
- Radiative flux at the ground is insensitive to ablation products because the core of the near wake region is mostly blackbody limited (see figure below)



Flow visualization of meteoroid entry environment

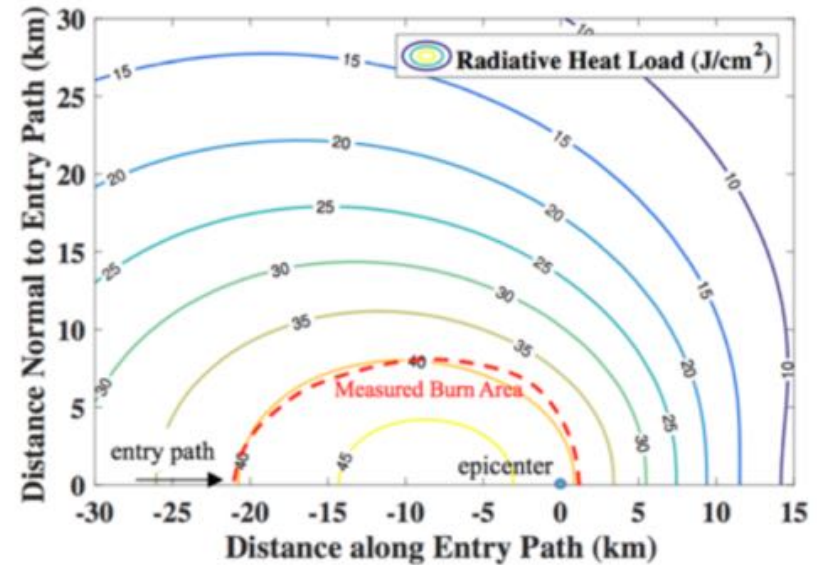


Spectra at two points along Ray 2 in the near-wake

Tunguska Thermal Radiation

An analytical model for thermal flux on the ground has been developed using the database of high-fidelity calculations

- This model can be readily input into analytical entry trajectory codes to perform risk assessments
- Good agreement for Tunguska was achieved using 18.5 km/s entry velocity, 60m initial diameter, and 30deg entry angle (see figure).
- Offset of the max thermal load from the blastwave epicenter its well captured



Comparison of predicted burn area to observation

$$q_{ground} = (2.75 + 0.16\phi) \left(\frac{R}{25}\right)^{1.7} \left(\frac{10}{L}\right)^2 \exp(4.1267 - 0.0357V - 54.137/V)$$

Empirical relation for thermal heating from asteroid airbursts